Physio-mechanical performance of super absorbent polymer modified low calcium fly ash-based geopolymer concrete against various curing regimes

BY

Muhammad Abdullah

FALL 2020-MS STRUCTURAL ENGG
00000328870

A thesis submitted in partial fulfillment of the requirements for the degree of

Master of Science in Structural Engineering

Department of Structural Engineering

NUST Institute of Civil Engineering (NICE)

School of Civil and Environmental Engineering (SCEE) National

University of Sciences and Technology (NUST)

H-12 Sector, Islamabad, Pakistan

This is to certify that the

Thesis titled

Physio-mechanical performance of super absorbent polymer modified low calcium fly ash-based geopolymer concrete against various curing regimes

Submitted by

MUHAMMAD ABDULLAH

FALL 2020-MS STRUCTURAL ENGG 00000328870

has been accepted towards the partial fulfillment

of

the requirements

for

Master of Science in Structural Engineering

_____

Dr. Hammad Anis Khan

Assistant Professor

NUST Institute of Civil Engineering (NICE)

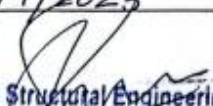**School of Civil and Environmental Engineering (SCEE)**

THESIS ACCEPTANCE CERTIFICATE

It is certified that final copy of MS thesis written by Mr. Muhammad Abdullah, Registration No. 00000328870, of MS Structural Engineering SCEE, (NICE), has been vetted by undersigned, found completed in all respects as per NUST Statutes/Regulations, is free of plagiarism, errors, and mistakes and is accepted as partial fulfilment for award of MS degree.
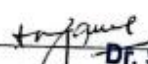
Signature: _____

Supervisor: Dr. Hammad Anis Khan

Date: 26/9/2023

Signature (HOD): HoD Structural Engineering
NUST Institute of Civil Engineering
School of Civil & Environmental Engineering
National University of Sciences and Technology

Date: 26-9-23

Signature (Associate Dean, NICE): _____

Dr. S. Muhammad Jamil
Associate Dean
NICE/SCEE, NUST

Date: 26/09

Signature (Principal & Dean): _____

11 OCT 2023   PROF DR MUHAMMAD IRFAN
Principal & Dean
Date: _____   SCEE, NUST

III

DECLARATION

I certify that this research work titled "**Physio-mechanical performance of super absorbent polymer modified low calcium fly ash-based geopolymer concrete against various curing regimes**" is my own work. The work has not been presented elsewhere for assessment. The material that has been used from other sources it has been properly acknowledge / referred.

Muhammad Abdullah
FALL 2020-MS STRUCTURAL ENGG 00000328870

PLAGIARISM DECLARATION

I-   I am aware of what plagiarism means and state that all the content in this paper, except for the parts that are properly acknowledged, has been created by me. I have used the Turnitin tool or a similar program to check for any similarities or originality issues, and I confirm that my supervisor has reviewed my report and that any problems identified have been resolved with their help.

II-   For referencing and citing sources, I followed the citation and referencing style, as outlined in the NUST Synopsis and Thesis Manual. I have given proper attribution to all significant ideas and quotations borrowed from other works or research in this dissertation, and they have been appropriately cited and referenced.

III-   I confirm that this dissertation has been solely produced by me.

IV-   I have not permitted, and will not permit, anyone to use my work with the intent of presenting it as their own.

Signature: _____   Date: _____

Student Name: Muhammad Abdullah

ACKNOWLEDGEMENT

Abstract

This research investigates the effect of internal curing (IC) with super absorbent polymer (SAP) on low calcium fly ash-based geopolymer concrete (GPC) with water, ambient and heat curing regimes. The impact of SAP on workability, shrinkages, physical, mechanical and microstructural properties of GPC are studied with three mixes (R0.5, R0.554, and S0.554). The liquid absorption of SAP was greater in water than the simulated alkaline solution of GPC. The SAP-modified mixture S0.554 has 0.3% SAP by weight of fly ash, and its effective alkali activator to fly ash ratio (AA/FA) is similar to mix R0.5, while its total AA/FA ratio is similar to mix R0.554. The results showed that inclusion SAP reduced shrinkage in GPC with comparable compressive strength and decreased workability. Additionally, at an equivalent effective AA/FA ratio, SAP increased compressive strength up to 7%. The flexural and tensile strength were enhanced along with physical properties by incorporating SAP as it densified the microstructure, which was proved by scanning electron microscopy (SEM) and X-ray diffraction (XRD). The performance of SAP was better when GPCs were ambient cured compared to water and heat curing.

Table of Content

List of Abbreviations

GPC	Geopolymer Concrete
GP	Granite Pulver
SAP	Super Absorbant Polymer
AE	Air-Entraining
w/c	Water to cement ratio
w/b	Water to binder ratio
AA	Alkali Activator
AA/FA	Alkali activator/Flyash ratio
SUHPP	Sustainable Ultra-High-Performance Paste
UHPC	Ultra-High-Performance Paste
HPC	High-Performance concrete
AS	Autogenous Shrinkage
DS	Drying Shrinkage
BPC	Belite rich Cement
CH	Calcium hydroxide
OPC	Ordinary Portland cement
IC	Internal curing
LWA	Light weight aggregate
RHA	Rice husk ash
CSH	Calcium silicate hydrate
GPM	Geopolymer mortars
AAFS	Alkali-activated fly-ash/slage
AAS	Alkali activated slag

RH	Relative humidity
GGBS	Ground granulated blast furnace slag
SEM	Scanning Electron Microscope
XRD	X-ray Diffraction
FA	fly ash
SF	Silica fume
CASH/NASH	Calcium/Sodium-Aluminate-Silicate Hydrate

List of Tables

List of Figures

Chapter 1

1. Introduction

1.1   Background

Climate change is harming the environment of the earth to a great extent, more aggressively than previously thought [1]. The average temperature rise per year, in the world, is increasing exponentially [2]. Human activities are the main cause of producing greenhouse gases, like carbon dioxide, which results in rapid climate change [3]. Infrastructure development is also one of the activities that are expanding rapidly and concrete after water is now the most used material on planet earth [4]. Due to low cost, better properties, and easy availability of ingredients, concrete is generally preferred for construction [5].

1.2   Environmental impact of concrete and its replacement

The endless development in the construction industry consumes a lot of energy and natural resources [6], along with the increased production of Ordinary Portland cement (OPC) [7]. However, OPC is not environment-friendly because its production causes the emission of greenhouse gases and consequently results in global warming [8]. The construction sector is recognized as a major source of carbon emissions [9] and it is predicted that 6 Giga tonnes of cement will be produced per year by 2056 [10]. Manufacturing 1.5 tonnes of cement requires 10 MJ of energy and releases around 1.2 tonnes of CO_2 [11]. Therefore, about 5–7 percent of CO_2 emission comes from the production of OPC, worldwide [12].

This negative environmental effect can be reduced by using alternate binders instead of cement like fly ash and blast furnace slag [13]. Geopolymer concrete (GPC), which is an aluminosilicate inorganic polymer, first described by Davidovits in 1979 [7] has been studied comprehensively for many years to validate its ability as a building material. A lot of research has been done on fly ash-based GPC earlier and more is ongoing [14]. GPC consumes less energy and natural resource. GPC replaces 100 percent OPC with improved mechanical and durability properties than conventional concrete [15]–[17].

1.3   Problem Statement

Geopolymer (GP) systems undergo severe shrinkage that causes the volume instability of concrete, resulting in cracks that make it susceptible to external factors [18]–[20]. Neupane et al. [18] found that the drying shrinkage of geopolymer concrete is comparable to that of OPC concrete. In alkali-activated (AA) systems, shrinkage has a significant effect on early-age cracking, as shown by Rodrigue et al. [19]. Wang and Ma [20] studied the effect of an alkali-activated fly ash/slag (AAFS) blended system revealed that using more than 70% fly ash results in a higher shrinkage rate. Researchers are aiming to develop an ambient cured GPC with reduced shrinkage stresses [21]–[26].

For OPC concrete, water and moist curing are standard curing procedures. Contrarily, due to its harmful impact on strength, the water curing procedure is rarely used for AAMs. In water curing of GPC, the alkaline solution will get diluted because of the water that has been absorbed [27]. One of the main benefits of using an ambient curing regime is that it can be used to easily replicate the on-site curing of OPC concrete at absolutely no additional cost [28]. In contrast, fly ash-based AAMs worked better in heat curing compared to ambient curing, which limited their wide range of applications [29], [30]. In fly ash-based AAMs, porosity and water absorption are greater by ambient curing and lesser by heat curing. Compared to GPC specimens that were heat-cured, ambient-cured GPC exhibits more shrinkage. When relieved at room temperature, fly ash-based GPC is thought to have a slight disadvantage due to its lower strength development [31] due to low reactive binders such as fly ash with low calcium content. The high temperature in this curing method serves as an accelerator to raise the chemical reactivity in the mixture matrix, mainly in the early ages [32]. Heating can greatly boost the early strength growth and decrease the early porosity of a mixture by increasing the alkaline activation and early hardening state features [33], [34]. However, the mass production of geopolymers can be significantly impacted by the elevated temperature curing [35], [36]. Moreover, the workers' safety is likewise susceptible to change. This has restricted the usage of GPCs.

Despite the superior strength of GPC, the necessity of high curing temperatures, as well as the use and storage of alkali solutions, must be addressed [9], [10], [37]–[40]. Ambient curing of FA-based GPC results in lesser strengths than curing in heat [41]. Researchers are aiming to develop

an ambient cured GPC that also possesses self-compacting concrete capabilities, which was developed in the 1980s by Okamura [21]–[26].

1.4   Research Objectives

Extensive research has been conducted on OPC systems, ultra-high strength concrete and alkali activated binders incorporating SAP to reduce the shrinkage. However, the influence of IC using SAP on the physio-mechanical properties of GPC along with other external curing techniques e.g. water, ambient and heat curing have not been sufficiently studied. Thus, the purpose of this research is to examine how SAP can act as an IC agent to decrease the shrinkage of low calcium fly ash-based geopolymer concrete. The current study looked at the variations in physiological properties of GPC subjected to water, ambient and heat curing with and without SAP. The objective of this research was to find the efficiency of SAP with respect to the curing mechanism and to find a more effective way of curing GPC that can enhance its strength by reducing shrinkage and promoting better microstructure.

1.5   Research Significance

The environmental hazards associated with the production of Ordinary Portland Cement (OPC) are widely recognized. OPC accounts for approximately 5-7% of the total global CO_2 emissions, making it a significant contributor to greenhouse gases and global warming. Geopolymer concrete, on the other hand, offers a cost-effective and environmentally conscious alternative to conventional concrete. Overall, this research provides valuable insights into the benefits and potential applications of internal curing with super absorbent polymers in low calcium fly ash-based geopolymer concrete. The findings contribute to the development of sustainable and high-performance geopolymer concrete materials with improved durability, reduced shrinkage, and enhanced mechanical properties.

1.6   Research Scope

The project was to cover the following:

- Evaluate density, workability, physical and mechanical strength and shrinkage of mixes.
- Find the influence of SAP in fly ash-based geopolymer concrete to be used.
- Evaluate properties of mix using different external curing methods

- Prepare an improved curing technique by incorporating SAP.

1.7 Thesis organization

The **first chapter** provides an introduction to the topic of the thesis, giving an overview of the research area and its significance. The **second chapter** presents a comprehensive literature review, discussing relevant studies and research conducted in the field. In the **third chapter**, various methods used for the characterization of super absorbent polymer (SAP) are presented. Additionally, it covers the standard methods and apparatus employed for conducting laboratory tests. Moving on to the **fourth chapter**, it presents the results obtained from the performed tests, along with a detailed analysis and reasoning behind them. The **fifth chapter** focuses on the discussions and interpretations of the results obtained from different tests. It provides an in-depth analysis and comparison of the findings, exploring their implications and significance. Finally, the **sixth chapter** concludes the thesis by summarizing the main findings, drawing conclusions based on the results, and providing recommendations for further research. The thesis concludes with a **reference section**, containing the cited sources and relevant literature used throughout the research.

Chaper 2

2. Literature Review

2.1 Introduction to Geopolymer Concrete

Geopolymer technology has shown promise in the transformation of industrial wastes into cement-free building materials. The geopolymers are made when alumino-silicate-rich industrial waste materials react with alkaline solutions [42], [43]. These industrial by-products (e.g., fly ash (FA), ground granulated blast furnace slag (GGBFS), silica fume (SF), etc.) exhibit binding properties like cement in presence of alkaline solutions (e.g., NaOH, KOH, Na_2SO_3, etc.), encouraging the sustainable use of materials. The aluminosilicate species dissolve in an alkaline solution quickly and condensates, producing a huge system of polymeric gels [44].

Successful use of GGBFS and FA in GPC lessens environmental impact by easy disposal of waste materials and contributes to the environmental benefits [45], [46]. ACI defines FA as the fine product produced from the combustion of coal. The properties of FA-based GPC are almost similar to conventional concrete [47]. GGBFS comes from iron and steel industries with a chemical composition similar to cement [48]. FA and GGBFS are the most effective industrial waste of all, used in GPC. The manufacturing of these industrial wastes is found to be increasing day by day and with the use of these materials, a steady geopolymeric interaction has been observed [49], [50]. Additional precursors like GGBFS can enhance fly ash-based GPC strength development and setting times [51]–[53].

2.2 Geopolymerization Reaction

The strength growth of geopolymers is not dependent on the formation of C-S-H (Calcium Silicate Hydrate) gels, but rather on compound phases such as C-A-S-H/N-A-S-H (Calcium/Sodium-Aluminate-Silicate Hydrate) or un-hydrated Na/Ca aluminium silicates such as C-A-S/N-A-S. As a result, industrial wastes with adequate proportions of silica and alumina, such as FA, GGBFS, silica fume (SF), or rice husk ash (RHA), could be employed as viable precursor materials for geopolymerization. [4]. These GPC base materials form cross-linked 3D aluminosilicate networks when they react with alkali activator solutions. These polymerization products reach significant strengths when the reaction is accelerated by curing at high temperatures [54]–[56].

2.3   Use of Geopolymer concrete for construction

In recent years, there has been a substantial increase in the use of GPC in construction activities in Australia. At Brisbane West Wellcamp Airport, the almost fifty-thousand-meter cube of GPC was cast on-site and utilized to make slip-formed pavement, which is the world's largest GPC operation to date. At the University of Queensland, Global Change Institute (GCI) is the first building to utilize precast GPC in structural components, while Pinkenba Wharf in Brisbane has 191 precast GPC decks designed to birth ships weighing up to forty thousand tonnes of weight. At Wyndham Street in Alexandria, Sydney, GPC forms a 3 x 15 square meters trial pavement portion., VicRoads has used it for several road infrastructure projects (Victoria State Roads Authority). VicRoads has designed guidelines for GP and alkali-activated materials (AAM), while the Cooperative Research Centres program (an Australian Government initiative) is constantly developing the 'Handbook for Design of GP and AAC Structures and performance-based designs being established. The literature also shows that this technology has been adapted and used in Russia, Ukraine, North America, South Africa, Poland, Belgium, the Netherlands, and the United Kingdom. These ongoing updates on geopolymer applications highlight the promise of geopolymer concrete delivery as a low-carbon approach [25], [43], [65]–[69], [57]–[64].

However, because of its restricted infrastructure uses, GP binder is still undervalued in the construction industry. There is a scarcity of literature that provides enough field application expertise for companies to get the trust they need in this new-generation binder [70].

2.4   Shrinkage and Self-desiccation

Shrinkage of concrete refers to the reduction in the volume of the concrete systems. There are various mechanisms of shrinkage like plastic shrinkage, chemical shrinkage, autogenous shrinkage, and drying shrinkage. Shrinkage without any external influence or aid is termed autogenous. Producing a drop in the internal relative humidity of the system by the removal of free water as a result of a chemical reaction to leave inadequate water amount to cover the surfaces of the solids is known as self-desiccation. The shrinkage which occurs due to chemical reactions is known as chemical shrinkage. The water loss by evaporation from the surface at an early age is called plastic shrinkage and at a later age is called drying shrinkage. As civil engineers, we should

be able to identify such shrinkage mechanisms but, in the end, we are more interested in the total amount of shrinkage of a given cement-based formulation.

2.5   Internal Curing techniques

The construction industry also generates a big quantity of water demand, and the external curing process wastes a large amount of water every day. Alternative water management approaches, such as self-curing mechanisms or internal curing, must be implemented to achieve long-term sustainability [71]. Internal curing is a way of reducing autogenous shrinkage in OPC binders by releasing water from the internal curing agent, into the matrix internally to keep a higher relative humidity [72]. Lightweight aggregates and superabsorbent polymers (SAP) are the two most used agents for internal curing. According to Jensen et al., SAPs have a cross-linked structure that allows absorbing water several times their weight [73]. The volume of SAP grows throughout the swelling phase when cavities are filled with water form. During concrete hardening, the extra water trapped in SAP is released into the environment, leaving the cavities as empty pores during later phases of hydration [74].

2.6   Use of Super Absorbent Polymer (SAP)

Quite recently, the use of SAP in construction materials has attained much attention from the research community. Extensive research has been carried out on OPC systems incorporating SAP. Dang et al. [75] observed that SAP can efficiently minimizes OPC concrete shrinkage and increases the concrete's ability to resist carbonation. Zheng et al. [76] reveal that Shrinkage and cracking can be reduced by adding SAP, as well as dimensional stability, freeze-thaw, and chloride penetration resistance can also be improved. Zhong et al., 2021 investigated that with the use of SAPs, we can prevent autogenous shrinkage. I. Kim et al. [77] found that drying Shrinkage and chloride penetration were also reduced with the addition of SAP. And many other researchers found that the addition of SAP improved the performance of OPC systems [78]–[81].

Scientists also added SAP to Alkali Activated (AA) systems. Song et al. [82] worked on alkali-activated slag (AAS) mortars containing SAP and their results showed that the loss in internal RH due to self-desiccation & autogenous shrinkage were both reduced due to the incorporation of SAP. The research of Tu et al. [83] on AAFS paste showed that IC by SAP can reduce the Chemical as well as autogenous shrinkage of AAFS, and the optimal SAP dose is found to be 0.3 percent.

Y. Wang et al. [84] concluded that the autogenous and drying shrinkage of AAFS paste and mortar can be greatly reduced with SAP. Li, Yao, et al. [85] confirm that the Autogenous shrinkage of AA Paste and mortar can be countered by SAPs.

Oh & Choi [86] showed that we could reduce the autogenous shrinkage of Alkali Activated Slag (AAS) mortar and paste with the addition of SAP. Similarly, Vafaei et al. [87], Jiang et al. [88] and Prabahar et al. [89] examined that the addition of SAP in AAS pastes minimizes autogenous shrinkage. As well as, Wang et al. [90] and Yang et al. [91] both found that in AAS, the addition of SAP reduces autogenous shrinkage. The effect of SAP and two expansive agents on minimizing the autogenous shrinkage of AAS mortars were investigated in their work by Jingbin Yang et al. [92]. Z. Yang et al. [91] [93] worked on AAS mortars and lessen the autogenous shrinkage and enhance the porosity, strength, and frost resistance. Afridi et al. [94] improved the resistance of GP mortar against chloride, acid, and sulfate attack by adding SAP. Previous research suggests that IC is beneficial not just for cement-based materials but also for Alkali Activated materials.

2.7 SAP in ordinary Portland cement concrete

When SAP is added, it has been demonstrated that the water & oxygen diffusion is maintained or enhanced. Similarly, the migration of chloride is minimized. The frost resistance with deicing salts is enhanced by SAP's production of air-filled voids compared to reference concrete which does not include SAP. It can be compared to air-entraining agents in concrete [78].

Khaliq & Javaid [95] studied different curing techniques and showed that while air-cured specimens have a high initial compressive strength, they have achieved only 70% of the ultimate compressive strength, whereas water immersion curing cylinders have the maximum compressive strength. And light weight aggregate cured concrete has a more uniform and enhanced microstructural development, resulting in higher mechanical strength and durability. Internal SAP curing had a slower strength growth at first, but it was able to achieve the minimum stipulated compressive strength necessary in the field as per ACI.

The effects of SAP content, size, and water entrainment on OPC concrete workability, shrinkage, compressive strength, carbonation & chloride penetration resistance were investigated by Dang et al. [75]. The findings reveal that pre-wetting of SAP increases the slump, otherwise decreases the

slump. The compressive strengths of concrete with SAP in a drying curing were more than those and almost equal to those of reference concrete in a normal compared to the control specimen, at a later age. SAP efficiently minimizes concrete shrinkage and increases the concrete's ability to resist carbonation & chloride penetration. SAP can efficiently modify the pore structure and enhance the microstructure. The size of gel pores and tiny capillary holes increases when SAP is added to concrete, whereas the size of giant capillary pores and air pores decreases.

From 3 to 28 days, the pore structure of the impacted zone around SAP in OPC paste with w/c of 0.24 and 0.30 was studied by Yang et al. [79]. SAP particles used in this study were 1.5 to 2 millimeters in size. SAP did not influence the pore shape of the affected zone, but pore diameter and pore volume were changed, according to the findings. At later ages, the impacted zone had a larger critical pore diameter but a smaller pore volume. The pore structure parameters computed permeability and mechanical strength of the impacted zone were higher compared to the control matrix.

Under conventional curing conditions, the effect of SAP in varied particle sizes (0.15, 0.3, and 0.6 millimeters) and content (0.2, 0.4, and 0.6 percent by weight of cement) on the mechanical and physical characteristics of OPC concrete at different w/c ratios (0.3 & 0.37) is investigated by Zheng et al. [76]. Shrinkage and cracking were reduced. Dimensional stability, freeze-thaw, and chloride penetration resistance were also improved. In addition, the SAP can enhance microstructure and refine the pores of the concrete matrix. The effect of SAP on increasing the porosity of concrete. The SAP content and concrete mechanical properties have inverse relationships. With an increase in SAP particle size, the mechanical performance of concrete got better first and then it became not as good as the reference concrete. 0.3 mm particle size and 0.2 percent content were regarded as optimum to obtain the best properties of concrete. Shrinkage of concrete reduces with an increase in the concentration of SAP.

For internal curing, two SAPs (sodium acrylate polymer and acrylic acid polymer) were utilized, each with five distinct particle sizes in cement-based materials with a w/c ratio of 0.35. At various ages, the moisture diffusion regions of SAP were compared and analyzed by Tan et al. [80]. The impact of SAP moisture on the surrounding mechanical characteristics, micro-hardness, and cement hydration has been investigated. At 180 minutes after the initial setting and before the final

setting of the matrix, the swelled SAP in red ink was applied to the specimen. The addition of SAPs raises the hydration level and affects the crystal structure of CH. In addition, the presence of SAPs reduces the average size of alite crystals. They also enhanced the affected area while increasing compressive strength. Acrylic acid-based SAP with particle size passing from 200 mesh was found more effective as can be seen in Figure 2.1.

The effects of the two forms of SAP (retentive and non-retentive) on autogenous shrinkage and cement hydration were investigated by Zhong et al. [96]. Based on Powers' model, the quantity of extra water in cement pastes containing SAP was determined. The shape of cavities created by the two SAP types, as well as the development of the hydration products inside these cavities, were also monitored. The absorption of SAP in pastes is about two times that of free absorption (using tea-bag method). Water was only released once it was placed, and it stayed within the initial SAP-formed cavities, but on-demand caused by chemical shrinkage & self-desiccation, it was released pastes, thus both retentive and non-retentive SAPs performed similarly. Both SAPs can prevent autogenous shrinkage as shown in Figure 2.2, but when the water has been entirely lost, they will behave as voids.

I. Kim et al. [77] studied the influence of internal pores generated by SAPs in OPC was explored by assessing the air content, pore size distribution, slump, drying shrinkage, compressive strength, and chloride penetration depth of concrete mixed with air-entraining (AE) agent or SAP. 0, 1.0, 1.5, or 2.0 percent of the acrylic acid-based SAP with a size range of 38 to 100 micrometers was added by mass of cement and a w/c ratio of 40 or 50 percent was used. Sealed-curing and water-curing studies were undertaken separately at the time to assess the internal curing impact. SAPs will rise the air content of concrete. As the amount of SAP applied grew, the amount of Water Reducing Admixtures required rose. The inclusion of SAP resulted in a greater number of small pores. It is predicted that by modifying the size of the dry SAP, desirable pore sizes can be achieved inside the concrete. When the SAP concentration was 1.5 percent of the concrete mix and the w/c was 0.4, the compressive strength was the highest. The ideal SAP percentage in the concrete mix was 1.5 percent, with 2.0 percent or above harming workability and compressive strength. Drying Shrinkage and chloride penetration were also reduced with the addition of SAP.
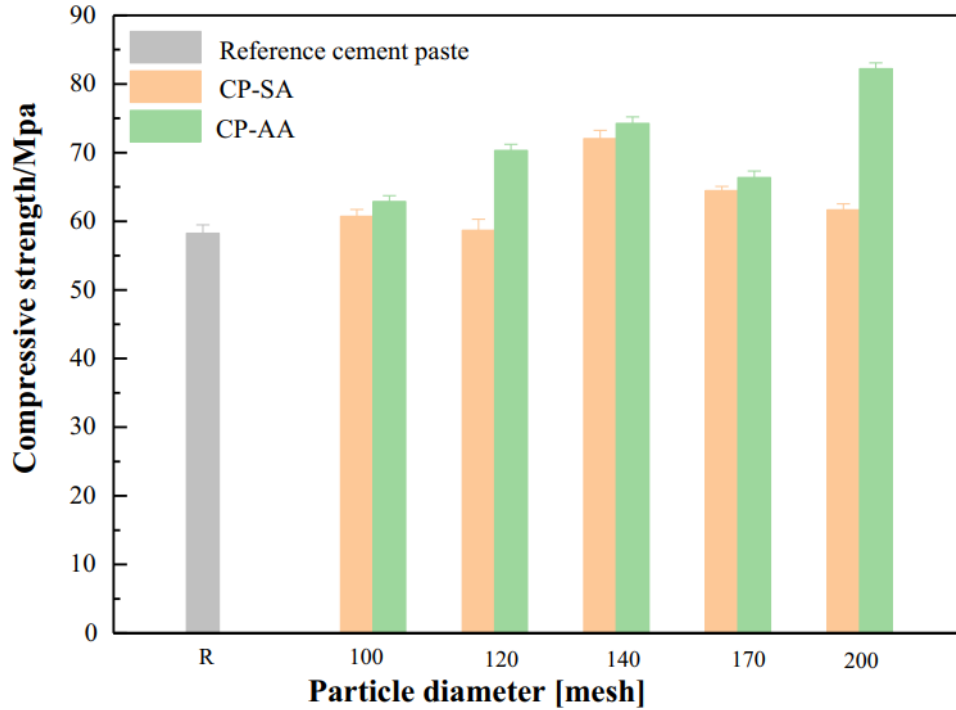
Figure 2.1. Compressive strength of cement paste after 28 days, containing SAP [80].
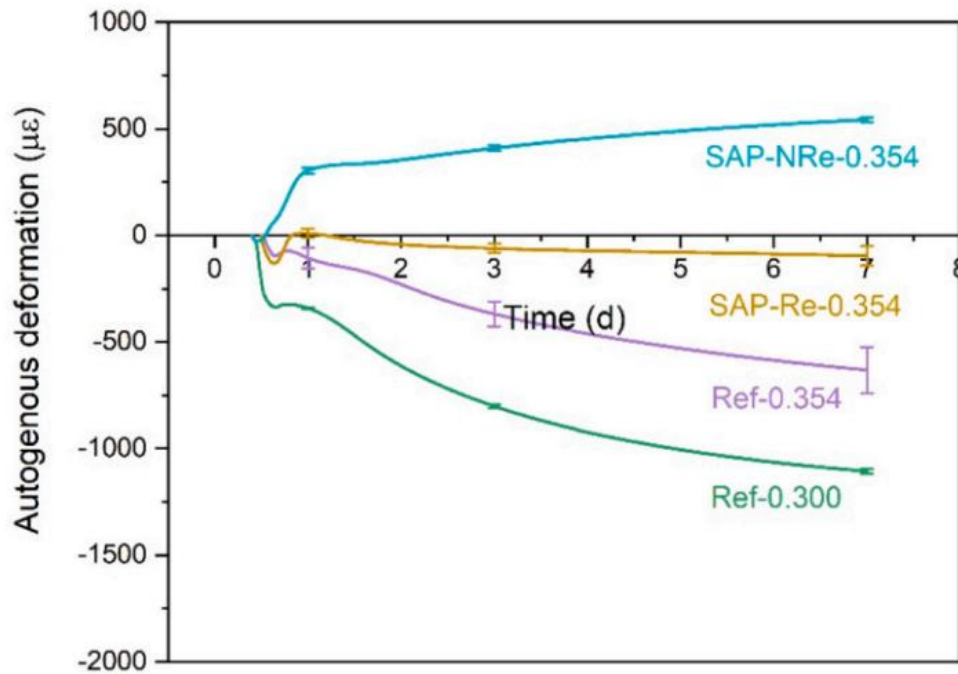
Figure 2.2. Autogenous shrinkage of cement pastes with retentive & non-retentive SAP.

Numbers after the dash represent the total w/c ratio [96].

I. S. Kim et al. [81] proposed a new method called the spin dry method for absorptivity measurement and compared it to the existing methods. The mechanical strength and resistance against freeze-thaw of mortar of ordinary Portland cement containing different types of SAP with different sizes were also studied. The SAP content was 0, 0.3, 0.6, & 0.9 percent by mass of cement with a w/c ratio of 0.45. Water curing and drying were done. The newly adopted method was found effective. In drying curing conditions, compressive strength was enhanced with the use of SAP. The w/c ratio used was much higher, otherwise better results can be achieved.

2.8 SAP in UHPC

Soliman & Nehdi [97] studied autogenous shrinkage and drying shrinkage in UHPC and the effect of both under changed drying temperature and relative humidity. Different mitigation methods are also adopted to compensate for that shrinkage. Cross-linked polyacrylic acid-based SAP with a size of 100 to 140 micrometers and 7 g /g absorption capacity was used. 0.6% SAP by mass of cement. SAP increased drying shrinkage, but autogenous shrinkage was reduced. The compressive strength of UHPC was found to be reduced with the addition of SAP. Compressive strength was dependent on the drying environment, particularly in cold regions where only lesser strength can be achieved.

Kong et al. [98] measured shrinkage and mechanical properties of HSC with pre-soaked SAP. The absorption capacity of SAP was found by using the teabag method and a 0.29 w/c ratio was used. SAP absorbs the water and expands and then releases that water and leaves large pores shown in Fig. which results in a reduction of strength due to a more porous microstructure. This negative effect of SAP can be minimized by using a suitable size and chemical composition of SAP but SAP induces voids as shown in Figure 2.3. He recommended that more emphasis should be given to the durability of concrete with SAP.

The influence of SAP of various sizes, contents, and additional water on permeability, drying shrinkage, and porosity with w/b ranging from 0.18 to 0.24 in high-performance cement-based materials were investigated by Ma et al. [99]. At the same effective w/b, SAP reduces strength. while increasing absorption, drying shrinkage, and chloride ion penetration and vice versa at the same total w/b which was used in the reference sample. The number of pores greater than 100 nanometres is reduced by SAP because the size of SAP voids is reduced as a result of the creation

of a hydration diffusion layer which in turn reduces the total surface and interior porosity. Although SAP void may be greater, larger SAP particles showed better results. The attributes of high-performance cement-based materials with the same total w/b in the comparatively drying environment are improved by the pore refinement and the reduction in evaporation rate produced due to SAP.

The impact of light weight aggregate internal curing on cracking sensitivity & shrinkage of High performance-concrete with reduced w/c ratios (0.33, 0.25, & 0.21) was investigated by Zhutovsky & Kovler [100]. Vacuum-saturated fine aggregate was used for internal curing. The drying shrinkage and cracking sensitivity were reduced when the w/c ratio was reduced but the total free shrinkage was reduced. Internal curing had a negative effect on the compressive strength of concrete. Splitting tensile strength was also reduced.

Kang et al. [101] evaluated the influence of different types of SAP on UHPC with different curing conditions. Water curing and air-drying conditions were used. The effect of internal RH on dimensional stability and compressive strength was measured. The strength development of concrete was found slow because SAP maintains a high RH inside the matrix. Large voids are formed due to SAP which reduces the concrete strength. The strength of concrete was negligibly affected when cured in air drying conditions compared to the control formulation. Shrinkage strains were reduced by using SAP.

The goal of Silva et al. [102] in their study was to see how different types of SAP (synthesis from different processes) affect the mechanical performance and autogenous shrinkage of fine-grained high-performance concrete. The Powers model was used to calculate the amount of water necessary for internal curing by SAP. The polymer was mixed dry with cement, sand, and silica fume mixture. Extra water required for internal curing and mixing water were both added at the same time. The findings reveal that all forms of SAP studied reduced autogenous shrinkage, but it compromises the compressive strength.

In the Ultra high performance-concrete samples cured differently (water and steam curing), SAP particles with different sizes and contents were added by Liu et al. [103] in his paper. As a result, the ITZ attributes of mechanical properties were assessed. The inclusion of SAP in UHPC has two effects on the ITZ. SAP thickened the ITZ and decreased cracking on drying due to internal curing,

although it left pores. SAP with a higher concentration or a bigger particle size intensified the negative effects of SAP on strength, which might be linked to the left holes caused by water desorption from SAP. When compared to water curing, steam curing improves the mechanical attributes of concrete, but not when it was compared with the control mix.

On the effectiveness of internal curing of UHPC mortar, the effects of SAP type (anionic & non-ionic), size (471.3 & 95.1 micrometers for ionic type), content (0.2, 0.4, & 0.6 percent), and pre-conditioning technique were explored by Liu, Farzadnia, Khayat, et al. [104]. Before mixing, the ionic SAPs were prewetted with more water (0.4 percent by mass). SAP can keep the RH high as shown in Figure 2.4. and decrease autogenous shrinkage, but it reduces compressive strength. At 90 days, smaller SAP particles showed an increase in compressive strength. With SAP, the total amount of heat emitted rose. Autogenous shrinkage was expedited due to pre-wetted SAP and caused hydration to be delayed.

The effect of 0.2 percent SAP and light weight aggregate on the strength and durability of rice husk ash-based high-performance concrete with a w/c ratio of 0.3 was investigated by Mudashiru et al. [105]. The use of SAP and LWA reduces autogenous shrinkage and improves compressive strength, but it also increases the porosity of the concrete matrix.

Xuan et al. [106] discover practical techniques for minimizing the Autogenous Shrinkage (AS) of a Sustainable Ultra-High-Performance Paste (SUHPP) containing an irregular shape SAP with a swelling capacity of 10.4 g/g and Belite Rich Cement. The w/b ratio was set to 0.2. By the mass of the binder, 0.25 and 0.5 percent SAP were added. In the first three days, a little content of SAP promotes strength, while Belite-rich Cement (BPC) can boost strength over the next 28 days. SAP reduces the AS but BPC specimens showed better results compared to other specimens. The combined water content, as well as calcium hydroxide (CH), increases, as SAP increases, having a positive effect on the hydration of cement but BPC reduces the amount of combined water and CH compared to the control specimen.
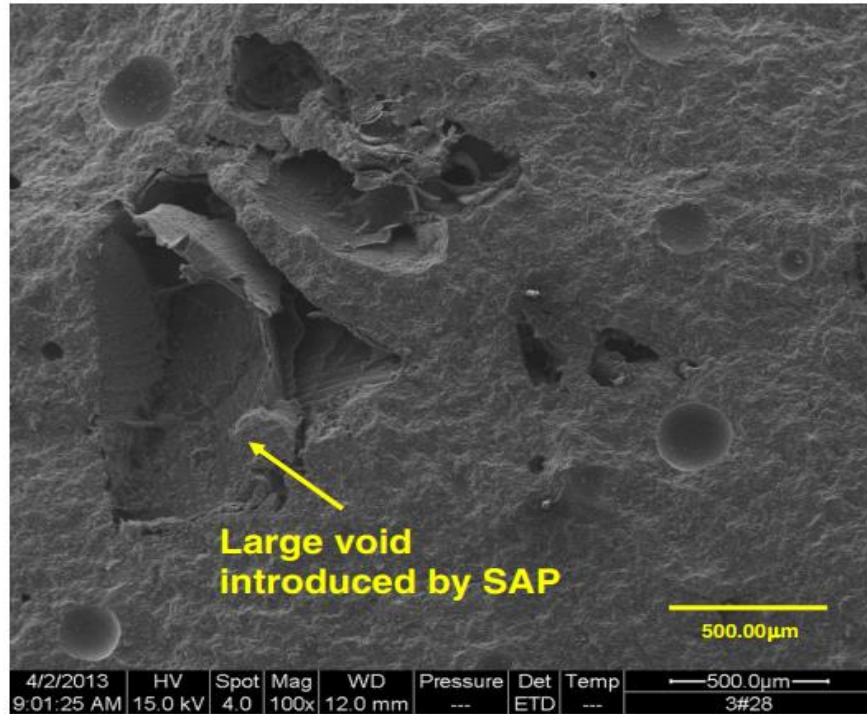
Figure 2.3. SEM picture of cement paste containing pre-soaked SAP after 28 days [98].
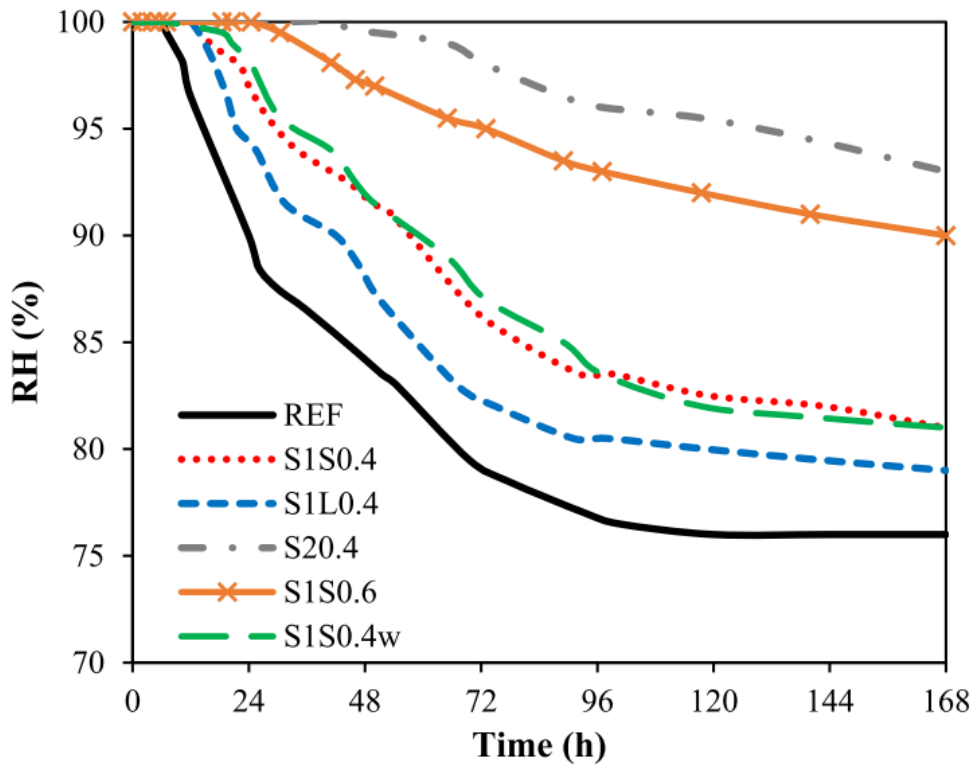
Figure 2.4. Influence of different SAP type on internal relative humidity of UHPC [104].

Compressive strength of HPC with w/b ratios ranging from 0.2 to 0.3, the effects of SAP size (300 & 600 millimeters), content (0, 0.2, 0.3, 0.4 percent by weight of binder), and binder type were investigated by Olawuyi et al. [107]. The effect of the binder type, on the other hand, was the most significant. When the combined impacts are taken into account, 0.3 of SAP concentration was the best for effective internal curing provision in HPCs, but compressive strength was reduced compared to the reference. The three impacting elements are w/b ratio, SAP dose, and particle size, in decreasing order of their effectiveness. In HPC, SAP inclusion of up to 0.3 percent with modest extra water was recommended. SAP addition reduced the density of concrete.

The influence of moisture gradient on Ultra-High-Performance Paste, microstructure, and hydration product at various levels from the surface exposed to drying, as well as a degree of hydration, density of CSH, and affected area by SAP, was investigated by Liu, Farzadnia, & Shi [108]. UHPC containing SAP has a higher total porosity than control UHPC, which acts as a weak spot and may diminish compressive strength. The inclusion of SAP enhanced hydration dynamics and allowed low-density C-S-H to be converted to high and ultra-high-density C-S-H. The impacted zone of SAP rose as the distance was increased from the drying surface, indicating that SAP is more effective in the inner layers.

2.9   SAP in Alkali Activated Concrete

The compressive strength, internal RH & autogenous shrinkage of alkali-activated slag (AAS) mortars containing various SAP doses and different alkali activators were all measured by Song et al. [82]. The SAP used was a cross-linked sodium polyacrylate. In the test, the average particle size of SAP was 412 micrometers was utilized. The quantity of extra water absorbed into the SAP was calculated based on its workability, such that the flow of the sample with SAP was the same as that of the sample without SAP. The loss in internal RH due to self-desiccation & autogenous shrinkage both reduced as the dose of SAPs rose, indicating that SAPs may be employed as internal curing agents efficiently, however, it created voids and impair compressive strength. The internal curing zone modeling that was proposed should be beneficial in calculating the proper dose of SAPs in AAS mortars.

Oh & Choi [86] wanted to see if superabsorbent polymers (SAPs) might be used as internal curing agents in OPC as well as alkali-activated slag (AAS) mortar and paste to reduce autogenous

shrinkage. The usage of different types of alkali activators with SAPs (avg. size of 220 micrometers) was examined. The SAP was irregularly shaped and made of cross-linked polyacrylic acid. Additional water was added to the SAP mixes to maintain equal flow as the non-SAP mixtures. The findings revealed that SAPs were effective in minimizing the shrinking of AAS mortars, which had previously been a major drawback in their use. When comparing AAS pastes containing SAPs to those without SAPs, higher decreases in porosity were found, but SAP reduces the strength at an early age. Isothermal calorimetry data for combinations with and without SAPs showed no significant differences. SAPs were important in holding water inside the matrix and allowing un-hydrated particles to be hydrated further. SAP also reduces the specific heat flow.

Internal curing of AAFS pastes made with class F fly ash and GGBS is studied by Tu et al. [83] using varied SAP doses (0 to 0.5 percent) and slag replacement (15 to 30 percent) to fly ash. SAP used was an irregularly shaped, cross-linked copolymer of acrylamide & potassium acrylate with a particle size of fewer than 300 micrometers. SAP absorption was found by examining the flow as a function of time. The flow of AAFS pastes is increased with the addition of SAP means that it increases the workability. Chemical & autogenous shrinkage of AAFS pastes are reduced by 18 to 45 percent and 76 to 85 percent, respectively, as the SAP dose is increased from 0.2 to 0.5 percent. But it compromises the compressive strength of AAFS pastes, the optimal SAP dose is found to be 0.3 percent. Internal SAP curing results in a reduced heat peak and a rightward displacement of the hydration peak due to that, the setting time of the AAFS paste was increased. This shows a decreased deformation (chemical shrinkage), which helps to mitigate autogenous shrinkage.

Two fly ash/slag ratios (50:50 and 70:30) paste and mortar are created by Y. Wang et al. [84] with two different doses (0.13 & 0.25 percent) of angular crosslinked anionic polyacrylamide SAP. The SAP raises the temperature of the alkali-activated pastes' reaction. The alkali-activated mortars' compressive strength is somewhat reduced by the SAP. The SAP greatly reduces the mortars' final autogenous shrinkage (> 50%) as well as their drying shrinkage (15 to 30 percent). As the SAP dosage is increased, shrinkage mitigation in the investigated mixes improves but it increases the mass loss.

In this study, SAP & metakaolin, are used to minimize autogenous shrinkage in fly ash & slag (almost 50 % each) based on alkali-activated paste and concrete by Li, Yao, et al. [85]. Acrylamide and acrylate cross-linked copolymers having particle sizes up to 200 micrometers were utilized. SAP at 0.16 weight percent and MK at 5 weight percent are recommended dosages. The results reveal that incorporating SAPs & metakaolin into Alkali activated paste and concrete greatly reduces cracking & autogenous shrinkage. Furthermore, the workability & strength of formulations containing SAP & metakaolin is improved.

Internal curing of alkali-activated fly-ash/slag (AAFS) paste with an irregular shape SAP of size under 200 micrometers is investigated in their work by Li et al. [109]. An equal amount of FA & Slag was used. Sodium hydroxide pellets & sodium silicate solution was used as an alkaline solution. The SAPs are shown to absorb liquid mostly before the paste's initial setting. Following that, the liquid is progressively released, keeping the paste's internal RH near 100%. Internal SAP curing can greatly reduce AAFS pastes autogenous shrinkage, particularly following the reaction's acceleration period. Internal curing's impact is due to the paste's reduced self-desiccation, rather than the creation of expanding crystals. Internal curing considerably reduces the cracking potential of AAFS under constrained conditions. Despite a small loss in elastic modulus & compressive strength, the paste's flexural strength has greatly improved which can be seen in Figure 2.5.

Li, Wyrzykowski, et al. [110] used Cross-linked acrylamide & acrylate SAP copolymers having size less then 500 micrometers and irregular shape, in their research. The teabag technique revealed that SAP had a much more absorption capacity in water compared to AA. Internal curing increased the total reaction degree and delayed setting times of AAS pastes by delaying peak of heat release rate. Internal SAP curing effectively counters the reduction in IRH and AS of AAS pastes caused by self-desiccation. The capability of AAS-paste shrinking when restrained to crack was also greatly decreased by SAP, however, they always have a negative impression on compressive strength.

The hardened & fresh characteristics of AAS paste with w/b ratio of 0.34 are controlled and improved using a modified poly Na-acrylate acrylamide type SAP composite supplemented with kaolin clay & micro silica were investigated by Fu et al. [111]. Two doses of SAP at a mass ratio

of 2.5 or 5 percent in relation to slag were adopted. The teabag technique is used to investigate the water retention & absorption capability of SAPs in different solutions. The conventional SAP had a negative impact on all of these attributes of AAS pastes, including setting, flowability and compressive strength. SAPs delayed the setting times. With increasing SAP dose from 2.5 to 5 percent, the range of 28-days compressive strength loss in AAS is between 17 to 32 percent. The usage of SAP enhanced with kaolin clay & micro-silica could alleviate unfavorable impact of SAPs commonly used on mentioned characteristics of AAS to a degree. At first, the addition of SAP composites reduces the drying shrinkage of AAS pastes; nevertheless, as time goes on, the DS of SAP-modified AAS becomes bigger compared to control specimen. Lower bulk stiffness AAS cured with SAP due to porosity expansion is most likely to blame this effect on drying shrinkage.
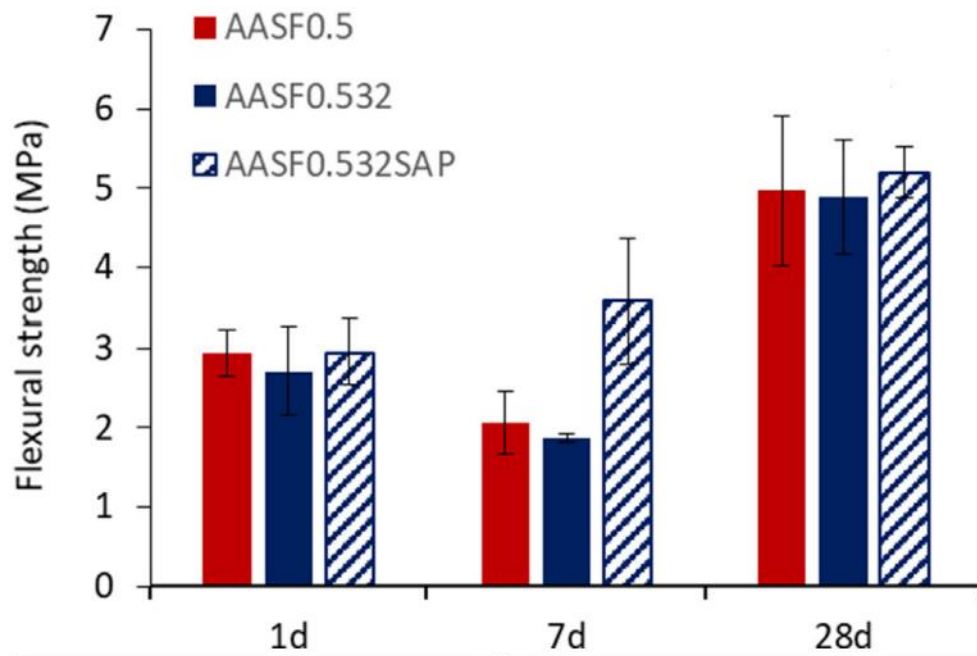
Figure 2.5. AASF pastes flexural strength [109].

Vafaei et al. [87] examined the impact of SAP on OPC and alkali-activated slag pastes' properties. 0.3 percent sodium polyacrylate SAP with an angular form manufactured with a particle size of around 200um was used. The SAP's absorption was determined from the teabag technique and AA were utilized. The flow values was compared to calculate amount of water that had been absorbed by SAP. When pore solutions obtained by AAS pastes were related to those recovered

by OPC paste, SAP showed greater absorption. The addition of SAP to AAS and OPC pastes proved beneficial in minimizing autogenous shrinkage. The positive impact of SAP on shrinkage. AS was greater in AAS compared to OPC paste. Due to presence of macro-voids, the compressive strength of SAP-modifies was lower than AAS pastes having no SAP. Electrical resistivity was lower in AAS pastes with SAP than in AAS pastes without SAP. This tendency is attributed to an increase in total w/b in AAS pastes with SAP.

The purpose of Wang et al. [90] was to see how SAP internal curing affected the AS, compressive strength, setting time, microstructure, & porosity of slag-based AAS mortars with 0.5 activators to binder ratio. A crosslinked sodium polyacrylate SAP size ranging from 300 to 500 micrometers was utilized at varying concentrations of 0, 0.05, 0.1, 0.2, 0.3, 0.4, & 0.5 percent by slag weight. The flow method was used to find the amount of extra water. Due to the extra activator produced from SAP, initial & final setting times of AAS pastes delayed by around 30 minutes & 10 minutes, respectively, with an increase in SAP dose. AAS mortars produced four to six times reduced AS compared to reference specimen, after adding 0.05 or 0.1 percent SAP. The autogenous shrinkage was abolished when the SAP dose was greater than 0.2 percent. Although IC through SAP lowered compressive strength, this decrease (23 percent for 0.2 percent SAP at 56 days) was acceptable considering the critical function it performed in preventing autogenous shrinkage. With a modest expansion and a 15% drop in compressive strength, 0.2 percent SAP content has been deemed an ideal.

The liquid release & absorption behavior of SAPs in water glass-activated slag (WG-AAS), NaOH-activated slag (SH-AAS) and PC pastes were compared by Jingbin Yang et al. [112] using NMR having low field. Three different sizes of sodium polyacrylate-based SAPs (422, 246, and 136 micrometers) were employed, with 0.3 percent content added. SAP liquid absorption was higher in SH-AAS paste than in PC & WG-AAS pastes. Release of liquid was quicker, because of the greater concentration of Ca^{2+} in PC's pore fluid. Despite the fact that the Ca2+ concentration in the pore liquid was lesser in the AAS system, the concentration of Na^+ was significantly larger in PC-based system because of activator. In PC system, Ca^{2+} is a significant factor affecting SAP swelling, but in the AAS system, the SAP's swelling restriction was the consequence of a combination of Na^+ & Ca^{2+} actions, with sodium ion dominating. Premature water release by SAP

might have not assist attenuate AS, & sluggish release mechanism might have harmful effect to maintaining IRH & reduction in autogenous shrinkage.

The effects of SAP & 2 expansive additions (gypsum & MgO) on shrinkage properties of AAS mortars were investigated in their work by Jingbin Yang et al. [92]. SAP is based on sodium polyacrylate with particle sizes ranging from 60 to 800 micrometers and doses of 0.1, 0.3, and 0.5 percent by mass of GGBFS. SAP's absorption was determined by teabag technique. The quantity of extra mixing water was determined using 1 H low-field NMR. AAS's setting time was lengthened by SAP. By continually releasing water, the SAP minimized the reduction in internal RH induced by the consumption of free water during process of AAS hydration, considerably reducing AAS mortar's AA. At 14 days, the sample containing a 0.3 percent SAP dose had autogenous shrinkage of only around 25% of the control sample. Although SAP can harm strength in compression when countering AS. But, between 7 and 28 days, the mortar's compressive strength containing SAP rose higher compared to samples. When MgO and SAP were added combined, AS was reduced more effectively. The SAP, on the other hand, was less successful in terms of total shrinkage. loss of AAS mortar's mass during drying was increased, which might raise AAS's DS and offset some of the autogenous shrinkage decrease.

The influence of SAPs as an IC agent on hydration properties and AS properties of alkali-activated slag (AAS) pastes was examined by Jiang et al. [88]. The internal curing agent in this investigation was SAP in irregular and porous form manufactured of Na-polyacrylate having 372 micrometers size and a concentration of 0.3 percent in AAS paste. Nuclear magnetic resonance technique is employed to analyze release and absorption of liquid processes of SAP in different alkali activator solutions of AAS pastes. The Teabag method was also used. As the silicate modulus rose from to 1.4 from 0.8, AS of AAS pastes containing SAP was reduced roughly by 80.6 to 70 percent. The SAP inclusion slowed exothermic 2nd peak but comulative heat of AAS pastes is increased. Furthermore, internal SAP curing may enhances slag reaction, predominantly for AAS pastes having greater silicate modulus, due to continual water and alkali activator solutions release from inside SAP as the hydration time increases. Furthermore, adding SAP to AAS pastes raised the pore volume & size of capillary pore, resulting in a loss in compressive strength. The SEM images are shown in Figure 2.6.
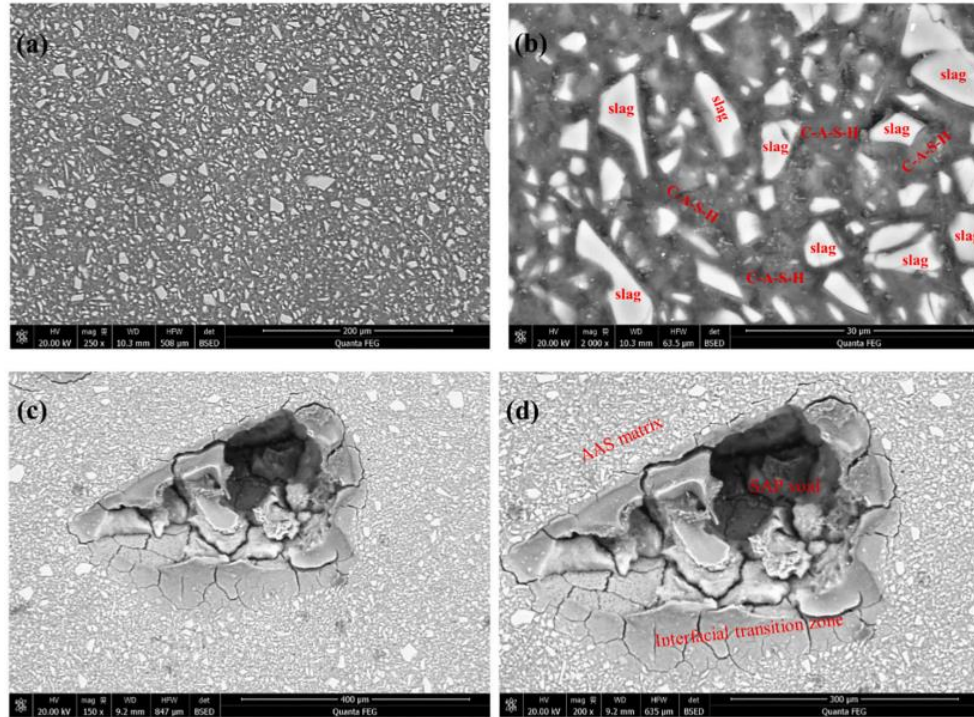
Figure 2.6. BSE images (a & b) without SAP & (c-d) With SAP [88].

Yang et al. [91] looked into the effects of varied liquid-binder ratios for IC and dry and wet mixing of SAP in alkali-activated slag mortar. Polyacrylic acid SAP of 10 to 1000 micrometers size was employed. The SAP's absorption capacity was determined using teabag technique. SAP absorbs substantially lower amount of fluid at higher AAS supernatant compared to water, according to the findings. When SAP is mixed with fluid firstly, it has a higher absorption than when it is mixed with solid first. If no additional fluid is incorporated, SAP lowers setting time & flowability of the AAS mortar. The setting time and flowability improve as the liquid-binder ratio (0.03, 0.06, and 0.09) is increased, but the decrease in compressive strength was found. Furthermore, samples mixed mixed have longer set time compared to samples mixed wett, despite the fact that their flowability & strength are polar opposites. Even with an extra having 0.09 l/b ratio, strength of IC-mixes is higher compared to the standard. The reason for this is that internal curing refines capillary & gel pores, despite the existence of huge spaces caused by SAP. SAP's addition reduces AS of AAS-paste greatly, but the further mitigating influence of the increased l/b ratio is minimal.

2.10   SAP in other concrete types

Uddin et al. [113] looked at the usage of SAP in different concentrations (0.2, 0.3, 0.4, percent by cement weight) to achieve IC & crack sealing in a Portland pozzolana cement with 2 percent fly ash replacement. With the addition of 0.3 percent, which was found to be optimum, the appropriate Slump (50 to 100) value was reached. The 0.3 percent SAP concrete has a lesser strength than conventional concrete after 7 days. We found that the weight loss of concrete with SAP was lesser than the initial weight loss when immersed in acid, indicating that it is more durable. The concrete swells at SAP, causing the shrinkage cracks to be stopped by reducing the cracks. Granite Pulver concrete blends were examined with the addition of SAP, which aids in internal curing by Rajamony Laila et al. [114]. The optimum percentages for SAP & GP, alonge with mechanical properties, were evaluated. GP was replaced with cement 5, 10, 15, and 20 percent by weight, and SAP was added in 0.1 to 1% by volume in each concrete mixture. The workability reduces as the amounts of GP and SAP grow. Some combinations showed an increase in compressive strength. Internal curing with GP-concrete blends of 0.3 and 0.4 percent SAP is favorable for achieving target strength. Most of GP-concrete mixes had tensile and flexural strengths that were nearly equal to the control mixture's strength. When 0.3 percent SAP was added, there were considerable improvement in flexural and tensile strength. SAP enhances the Elastic Modulus at a lower concentration.

2.11   SAP in Geopolymer

The durability of GPMs containing SAP against chloride, sulfate & acid was investigated in their work by Afridi et al. [94]. GPMs with different water/solid & sand/FA ratios were made using class-F fly ash, and AA was a mixture of Na_2SiO_3 and NaOH solutions. The SAP (0,1,2 percent by weight of binder) used in this study was a x-linked polyacrylic acid and polyvinyl alcohol copolymer with a size of approximately 350 to 450 micrometers. All samples were first heat cured at 80°C, before being cured at room temperature. The weight lost and compressive strength of samples were utilized to extract durability resistance of GPMs. On the microstructure of GPMs, SAP has a protective impact by reducing the porosity. It aids in the attainment of a higher degree of geopolymerisation and enhances the microstructure of GPMs. As a result, while this effort is likely to help more sustainable and durable GPMs GP-concrete manufacturing, it compromises the compressive strength.

Chapter 3

3. Materials and Testing Methods

3.1 Raw Materials

To prepare GPC, class F fly ash as per ASTM C-618 [115] was used as the primary precursor and was obtained from Coal Power Plant in Sahiwal, Pakistan. X-ray fluorescence (XRF) was carried out to obtain the chemical composition of fly ash as displayed in Table 3.1 The chemical composition of fly ash determined by XRF analysis.. Blended mixtures of fly ash were prepared with alkaline solution, coarse aggregate, and fine aggregate. The primary properties of fly ash are seen to comply with the guidelines for fly ash established by Fernández-Jiménez & Palomo [116], i.e., a carbon content percentage lower than 3 wt% and a content of Fe_2O_3 not exceeding 10 wt%. In addition to having a relatively low Ca concentration, the Si to Al molar ratio was around 1.92. The density of fly ash was 2.25 g/cm^3.

The locally available limestone - based coarse aggregates were used with a maximum size of 12.5 mm. The apparent specific gravity of coarse aggregates was found 2.66 and the water absorption was 1.34% as per ASTM C-127 [117]. Lawrencepur sand was used as the fine aggregate, having a fineness modulus of 2.3 according to ASTM C-136 [118] and an apparent specific gravity of 2.62 with 2.3% water absorption determined by ASTM C128 [119]. Prior to use, both aggregates were initially oven dried at 100 °C for 24 h. As a result, the aggregate that was later saturated surface dried (SSD) before mixing had all its moisture removed.

Table 3.1 The chemical composition of fly ash determined by XRF analysis.

Moisture	SiO_2 (Silica)	Al_2O_3 (Alumina)	Fe_2O_3 (Iron Oxide)	CaO (Lime)	MgO (Magnesia)	SO_3 (Sulphuric Anhydride)	LOI (Loss on Ignition)
0.19	50.22	26.2	0.88	3.94	1.6	0.56	2.8

The activator solution was an alkaline mixture of sodium hydroxide (NaOH) and sodium silicate (Na_2SiO_3). NaOH was in the form of pellet with purity of 99%. The NaOH solution was prepared by adding these pellets to water. For 14 molar NaOH solution, 40% solid pellets and 60% water was added. This concentration was chosen after preliminary research by Ghafoor et al. [120], according to which the molarity of the NaOH solution at which the alkali-activated geopolymer showed its best mechanical performance was 14. Na_2SiO_3 solution consisting of 55% water and

45% solids were obtained from Peshawar Chemicals Pakistan. The solids consist of 11.3% Soda Ash (Na_2O) & 33.7% Silica sand (SiO_2) having 3 modulus ratio (M_s; $M_s = SiO_2/Na_2O = 3$).

All three GPC mixtures were made with a constant NaOH molarity of 14 and a Na_2SiO_3/NaOH ratio of 1.5 (by mass) to achieve the optimum mechanical strength [120]. Note that the blended alkaline activator was made 24 h before casting of GPC in order to allow the mixture cool and adjust to the ambient environment. SAP used in this study was sodium polyacrylate having an irregular shape as shown in Figure 3.1 obtained from a local vendor.

3.2   Mix Proportion, batching and curing techniques

Three GPC mixtures, each consisting of 368 kg/m^3 of fly ash, were prepared as per [120], two of which were referred to as R0.5 and R0.554, while the third one, which included SAP, was named S0.554. The mass ratio of alkali activator to fly ash (AA/FA) for R0.5 was 0.5, and for R0.554 and S0.554 it was 0.554. Additionally, S0.554 contained 0.3% SAP consistent with the literature [83], [86]–[88]. The extra amount of activator was determined based on the absorption capacity and SAP content (SAP absorption x SAP content = 18 x 0.3% = 0.054) that was added to SAP-modified formulation to compare the effect of extra activator as well. S0.554 had a total AA/FA ratio of 0.554, with an effective AA/FA ratio of 0.5, (effective AA/FA ratio representing the available amount of free activator during mixing.) Both R0.5 and S0.554 had the same effective AA/FA ratio, while R0.554 had the same total AA/FA ratio as S0.554. Hence, we can analyse the impact of additional activator present in S0.554.

The ingredients were blended in the Hobart mixer. Two minutes of dry mixing (60 rpm) followed by six minutes of wet mixing time was according to Liu et al. [121]. SAP was added during dry mixing. The addition of 90 percent alkali solution followed by mixing (120 rpm) for 180 sec. Addition of 10 percent extra water and 10 percent alkali solution followed by mixing (120 rpm) for 180 sec as shown in Figure 3.2. Then the GPC was poured into moulds and cylinders with 3 layers and every layer was compacted by using a mechanical vibrator. The samples were demoulded after 24 h and cured for 28 days. Cylindrical samples of 100 mm diameter with 200 heights and prisms of 100 x 100 mm^2 x-section with 500 mm length were prepared.

Later, the samples were cured for 28 days under three distinct conditions as labelled in Figure 3.3, resulting in a total of nine formulations, which are presented in Table 3.2. For ambient curing, the specimens were enclosed in plastic sheet and kept at room temperature. Similarly, for heat curing the samples were wrapped in plastic and placed in an oven at 80 °C for 24 hours and then placed it under ambient curing [94]. For water curing, specimens were placed inside water. The IDs given to the specimens followed a specific pattern, where R represented reference specimens, S represented SAP-modified specimens, 0.5 or 0.554 represented the AA/FA ratio, and the last letter indicated the curing type (e.g., A for ambient curing). The first three mixes were labelled as R0.5, while the second and third groups of three mixes were labelled as R0.554 and S0.554, respectively.
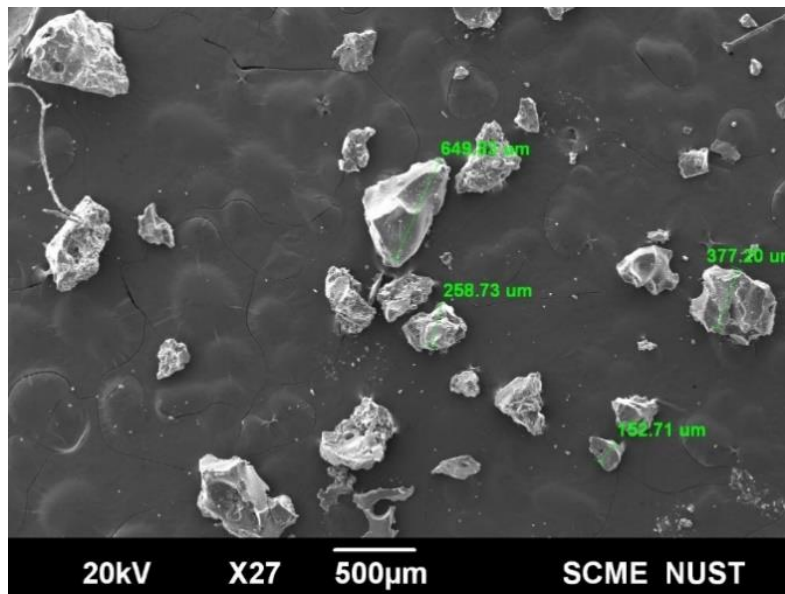
Figure 3.1. SEM image of dry SAP particles.

Table 3.2. Mix proportions of geopolymer concrete.

ID	FA (kg/m³)	Coarse Agg. (kg/m³)	Fine Agg. (kg/m³)	NaOH sol. (kg/m³)	Na₂SiO₃ sol. (kg/m³)	AA/FA	SAP (%)	Curing
R0.5-A	368	1294	554	73.6	110.4	0.5	0	Ambient
R0.5_H	368	1294	554	73.6	110.4	0.5	0	Heat
R0.5-W	368	1294	554	73.6	110.4	0.5	0	Water
R0.554-A	368	1294	554	73.6	110.4	0.554	0	Ambient
R0.554-H	368	1294	554	73.6	110.4	0.554	0	Heat
R0.554-W	368	1294	554	73.6	110.4	0.554	0	Water
S0.554-A	368	1294	554	73.6	110.4	0.554	0.3	Ambient
S0.554-H	368	1294	554	73.6	110.4	0.554	0.3	Heat
S0.554-W	368	1294	554	73.6	110.4	0.554	0.3	Water

Figure 3.2 Mixing procedure for GPCs.
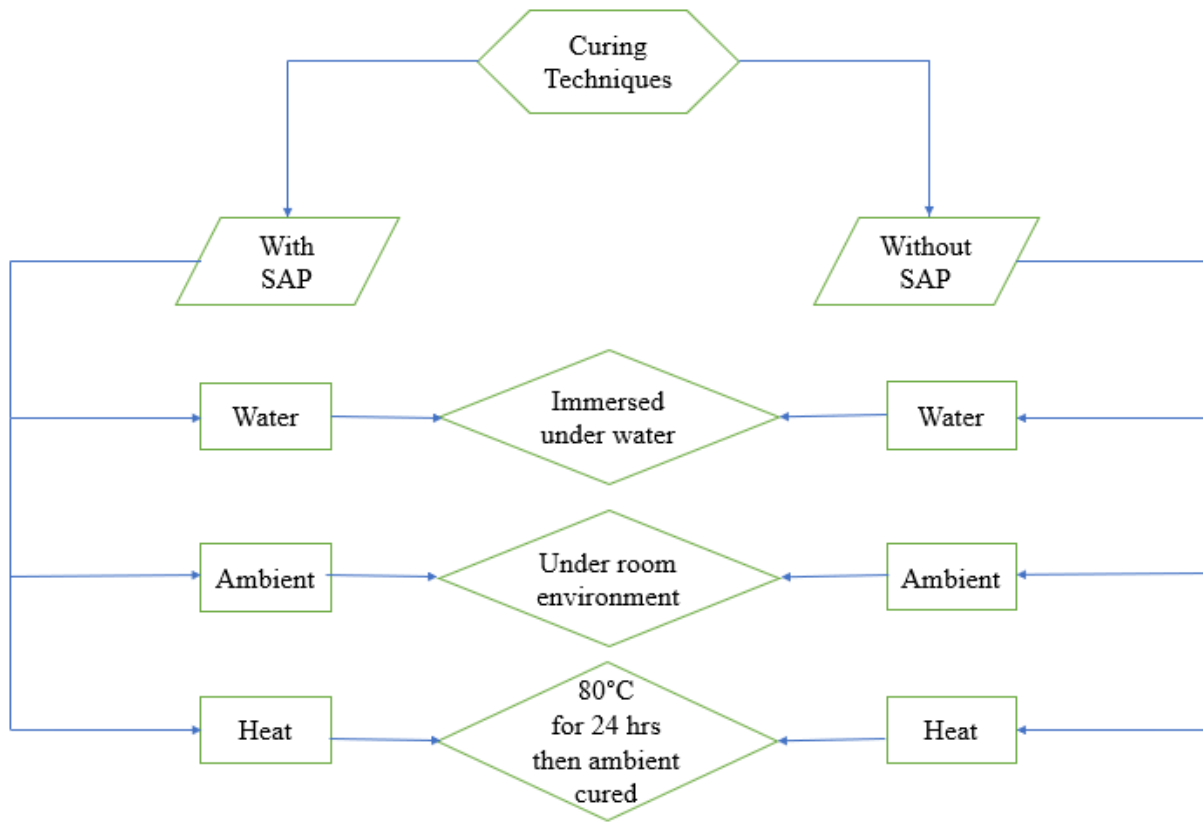
Figure 3.3. Different curing methods adopted for GPC.

3.3   Teabag Method

The Teabag method was used to determine the absorption capacity of SAP in this study as it is the most appropriate method for SAPs. To simulate a cementitious environment, a slurry was made by adding 20g of binder in 200 g of alkali activator. This solution was stirred and subsequently filtered to get the pore fluid.

In a teabag (mass m2) that had been pre-wetted in the equivalent liquid, 0.2 to 0.3 g of SAP particles (precise mass m1) were placed. A teabag containing SAP was suspended in a beaker holding the liquid of interest. To prevent carbonation and evaporation, the beaker is covered with a plastic sheet. The teabag with the SAP was released to be weighed after 30 seconds, 2, 5, 10, 15, 30, 60, and 180 minutes (mass m3).

To remove excess and poorly attached liquid, it was placed on a dry towel and rubbed with another dry cloth for about 30 seconds. Some of the liquid retained between the SAP particles as capillary water could escape the sample. The sample was not crushed, however, to preserve the polymers' storage function. According to the equation below, the amount of absorbed liquid concerning the initial mass of SAP was computed. [122]–[124].

$$mass\ of\ water = m = (m3 - m2 - m1)/m1$$

3.4   Workability

A slump cone test was conducted on samples as per ASTM C143 [125]. GPC was added to the cone in three layers and 25 blows were applied to each layer. Then the cone is raised and the geopolymer concrete is allowed to subside. The vertical distance between the top center of geopolymer concrete and the original cone top is measured with the help of a ruler, which is the slump value. Slump reading was noted subsequently with the help of a ruler as shown in Figure 3.4.

Figure 3.4. Workability test using slump cone apparatus.

3.5   Fresh Density

The wet density of freshly prepared concrete mix was calculated as per ASTM C138 [126]. Fresh mixture weight was measured using digital balance, divided by the volume of the cubical mould to get fresh paste densities. The samples were weighed again after curing and volume was determined by measuring dimensions with the help of a Vernier calliper for hardening density.

3.6   Density, Absorption, and Voids in Hardened GPC

The water absorption capacities of all the mixes were determined according to ASTM C642 [127]. After curing, cubes were oven dried at 100±5 °C for 24 h and weighed. Then cubes were kept in water for 24 hours and weighed in SSD conditions. Then samples were suspended in water with wire and apparent weight was measured. After measuring all the weights, the absorptions, densities, and voids were calculated. Then use the following equations to determine all the parameters.

Absorption after immersion, % = [(B-A)/A] *100

Absorption after immersion & boiling, % = [(C-A)/A] *100

Bulk density, dry = [A/(C-D)] * ρ *100

Bulk density after immersion = [B/(C-D)] * ρ *100

Bulk density after immersion & boiling = [C/(C-D)] * ρ *100

Apparent density = [A/(A-D)] * ρ *100

Volume of permeable voids, % = [(C-A)/(C-D)] *100

where:

A = Oven-dried mass of sample in air, in grams

B = Surface dry mass of the sample after immersion in air, in grams

C = Surface dry mass of the sample after immersion and boiling in air, in grams

D = Sample's apparent mass after immersion & boiling in water, in grams

ρ = Density of water = 1 g/cm^3

3.7   Mechanical Properties

The tests for compressive strength were performed on 7, 14, and 28 days cured samples, and an average of three samples was taken. ASTM C39 standard was followed [128]. Place the samples in the compression testing machine as shown in Figure 3.5 and applied at a loading rate of 0.25MPa/sec. The maximum (crushing) load applied to the specimen was recorded and the strength of the sample was evaluated.
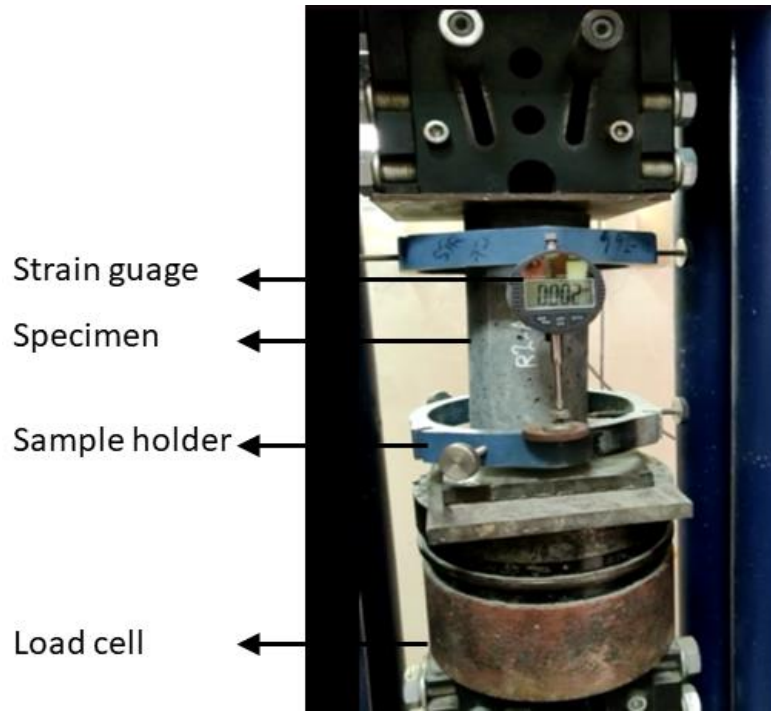
Figure 3.5. Compression testing machine.

While for the flexure strength test of concrete, beams of 100 x 100 x 500 mm^3 were cast. At the age 28th days, all formulations were tested in flexure according to standard ASTM C293 [129]. As shown in Figure 3.6, the specimen was placed in a flexure testing apparatus and a uniform loading rate of 1MPa/min for flexure was adopted. When the specimen was broken measure the dimensions of the specimen and calculate the modulus of rupture.
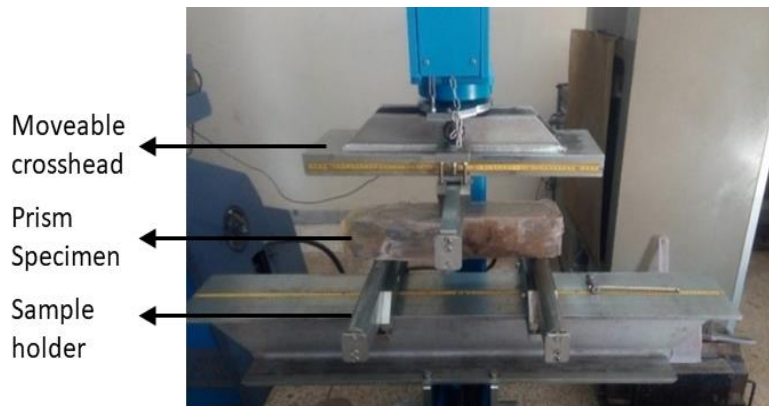
Figure 3.6. Flexural testing machine.

A split tensile test was carried out according to ASTM C496 [130] standards. The Universal Testing Machine and the splitting tensile apparatus were used as shown in Figure 3.7. The sample was mounted perpendicular to the direction of loading such that the load was acting along its whole length. No capping was done. The loading rate was kept at 0.02 MPa/s. The strength was noted at the cracking of the specimen.
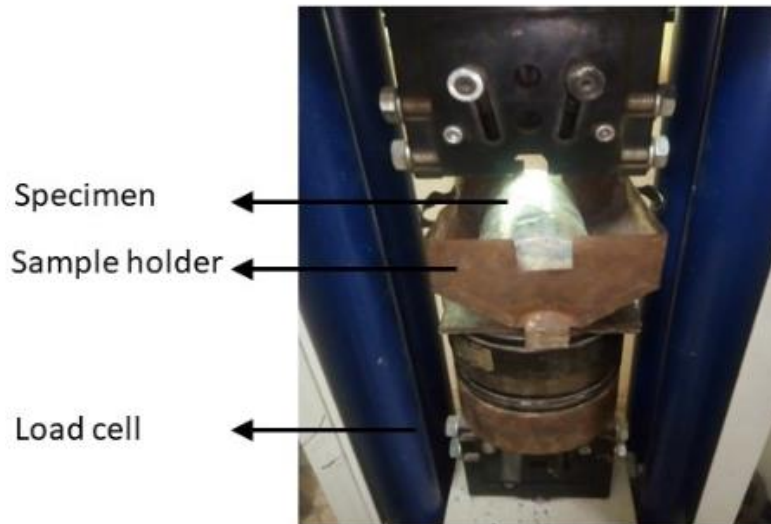
Figure 3.7. Split tensile test setup.

3.8 Shrinkage

The Shrinkage of GPC was found by measuring the change in length as per ASTM C157. Three concrete prisms of 100 x 100 mm^2 x-section with a length of 285 mm were prepared for each formulation. Concrete was poured into the moulds in two equal layers and each layer is compacted. After 24 hours of casting, samples were demoulded. The length of samples was recorded immediately after demoulding, as well as at 1, 2, 4, 7, 14 & 28 days. The change in lengths was calculated and shrinkage was measured [131]. To measure autogenous shrinkage samples were wrapped in plastic but for drying shrinkage, they were not wrapped as shown in Figure 3.8 [132].

Figure 3.8. (a) Samples for autogenous and drying shrinkage (b) Shrinkage test apparatus.

3.9 Bulk Electrical Resistivity

A cylindrical sample of 100mm diameter and 200mm length were prepared. According to ASTM C1760 [133], a simulated solution is prepared by first mixing 2 grams of calcium hydroxide, 7.6g of sodium hydroxide, and 10.64g of potassium hydroxide in dry form. After that deionized water was added to make a 1-liter total volume. After curing for 28 days, these samples were saturated in a simulated solution and then placed between the electrode plates in the Bulk Resistivity Test device shown in Figure 3.9. Start the apparatus and note the value of the applied voltage. After 2 to 5 sec, the value of the current was recorded. Repeat the measurements at least twice. Use the following equation to find the value of Bulk Resistivity in the unit of ohm-m.

$P=VA/IL$

where:

L = length of the specimen, in meters,

A = Cross-sectional Area, in m^2,

V = voltage in amperes,

33

and I = current in amperes,

Figure 3.9. (a) Bulk resistivity test apparatus (b) Electrode plates

3.10   Permeability

For three days, concrete cylinders were exposed to a water pressure of 0.5 N/mm^2 acting normally to the mould filling direction from below in the permeability test apparatus shown in Figure 3.10. Throughout the exam, this pressure must remain consistent. The test may be stopped if water gets through to the underside of the specimen, and the specimen may be rejected as failed. It was examined to see if and when the faces of the unexposed specimens develop symptoms of water infiltration. The specimen was withdrawn and split along the middle as soon as the pressure has been released, with the face that was exposed to water facing down. When the split faces began to dry (after about 5 to 10 minutes), the maximum depth of penetration in the slab thickness direction in mm was measured and the extent of water permeation was determined. The test result was the average of the highest depth of penetration obtained from the three specimens thus examined [134].

Figure 3.10. Permeability test apparatus.

3.11   Ultra-Sonic Pulse Velocity

This test was performed according to ASTM C597 [135] by UPV apparatus as shown in Figure 3.11. A coupling agent was applied on the surface of the specimen or the face of the transducer. Both transducers were attached to the specimen in a directly opposite direction and the pulse generator was started. The transducers were connected firmly against the concrete surface until we got a stable value of transit time. This time and length between the transducers were noted and the pulse velocity was calculated. Use the following formula to calculate the pulse velocity.

V = L/T

where:

V = pulse velocity in meter/sec,

L = distance b/w centers of transducer face in meters, and

T = transit time in seconds

Figure 3.11. Ultra-sonic pulse velocity test apparatus.

3.12   X-ray diffraction (XRD)

X-ray powder diffraction (XRD) is a rapid analytical technique primarily used for the identification of the phase of a crystalline material and also to provide information on the dimensions of a unit cell. The material to be analyzed is finely ground, homogenized, and the average bulk composition is determined. XRD was used to analyze the composition of hydration products of selected samples. Samples at 28 days were dried at 50 °C for 12 hrs and then crushed in powdered form. XRD was performed using a machine having Copper as a target. The scan range was 10-70 at 0.02/step.

3.13   Scanning Electron Microscopy (SEM)

To investigate the particle size, shape, and morphology of different constituents and also to study the hydration products, microstructure, and ITZ of formulations, scanning electron microscopy was carried out as per ASTM E1508 [136] and ASTM C1723 [137] as shown in Figure 3.12. Broken pieces of the sample were collected, and oven dried at 100±5 °C for 24 h to stop the hydration process using ethanol and make the samples free from moisture. Then samples were broken into required sizes (about 2 to 3 millimeters) and stuck with carbon tape on studs to obtain

clear and more perceivable images. Samples were coated with 20nm of gold to make them conductive using a sputter coater. SEM analysis was performed using the model "TESCAN VEGA3". The resolution of SEM images can be varied.

Figure 3.12. (a) Scanning electron micrograph apparatus (b) Samples (c) Gold plating of samples

Chapter 4

4. Results

4.1 Absorption and Releasing Capabilities of SAP

The water-absorbing ability of SAP was tested in an experiment, and the results of SAP absorption with time can be seen in Figure 4.1. The absorption curves in deionized water and simulated pore solution were also displayed for comparison. It was found that the absorption rate of SAP increased steadily for ten minutes before remaining constant. In this solution, SAP absorption began rapidly and peaked a few minutes after the SAP first came into contact with the solution. The maximum absorption capacity of SAP was accomplished within just 10 minutes, with 108 g/g of SAP in tap water and an impressive 18 g/g in simulated pore solution of GPC. This value was utilized to determine how much SAP was included in the mix design for the internally cured mixtures as described in section 3.2.

As can be shown, SAP has a significantly greater absorption capacity in water than it does in GPC supernatant. The adsorption procedure pursued a comparable pattern even though SAP absorption capacity varies in various aqueous solutions. These findings are in line with previous research conducted by Li, Wyrzykowski, et al. [110]. The alkaline environment of the simulated pore solution resulted in less absorption compared to tap water, proving that SAP is sensitive to the composition of the liquid it is exposed. The water-releasing capabilities of SAP were tested under different temperature conditions in this study. As depicted in Figure 4.2, it was discovered that SAP was able to release more water at higher temperatures, as the decrease in RH prompted the release of water into the environment, a phenomenon that has been previously reported Li, Zhang, et al. [109]. SAP releases more amount of liquid if kept for longer period of time (3 hours) at higher temperatures, which can be seen from Figure 4.3, It releases 45% absorbed water in one hour and more than 95% absorbed water in three hours at 100 ℃.
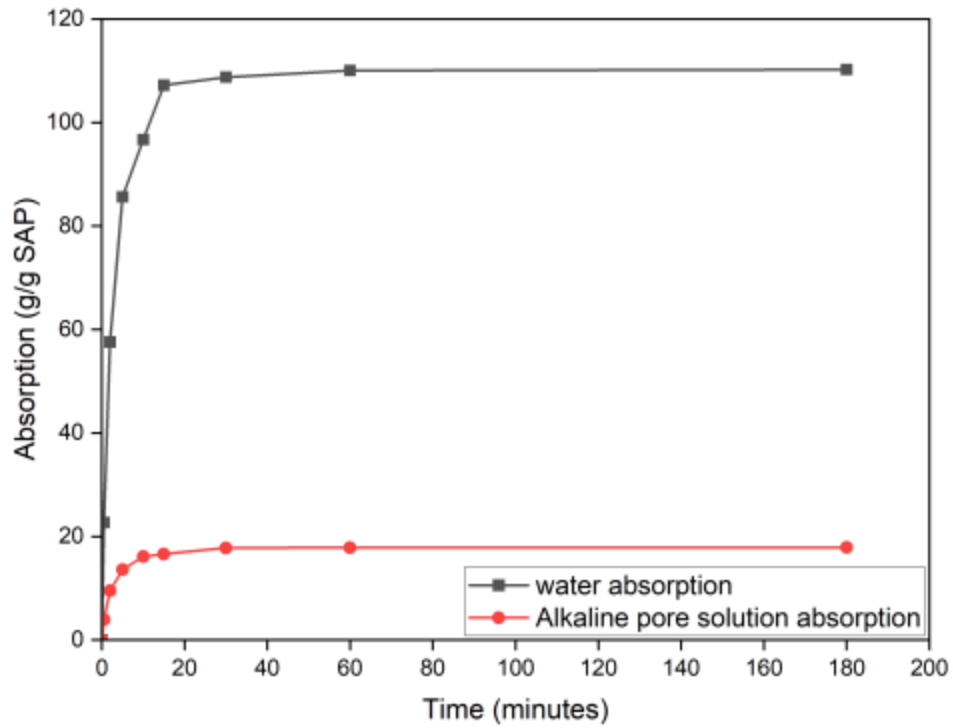
Figure 4.1. Absorption capacity of SAP in water and alkaline pore solution with time.
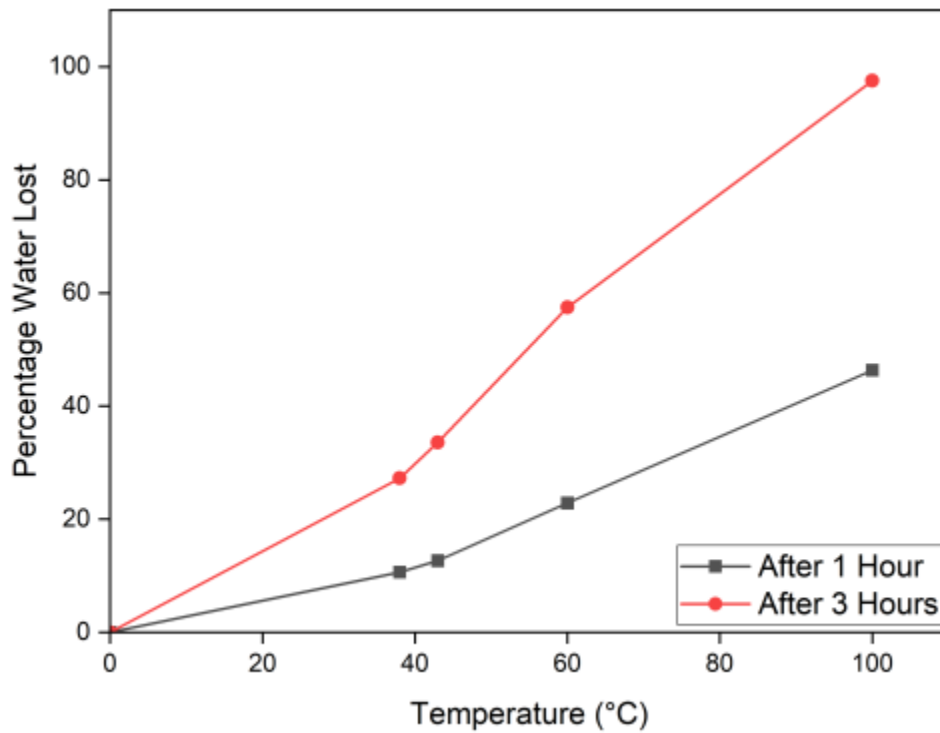
Figure 4.2. Percentage of water lost by SAP with an increase in temperature.

Additionally, when SAP exposed to sunlight over time at a temperature of 35 ± 5 ℃ , SAP was found to release an increasing amount of water, as shown in Figure 4.3. Almost 90% of the water immersed by SAP was emitted within just 8 hours under environmental condition, demonstrating the efficiency of SAP.
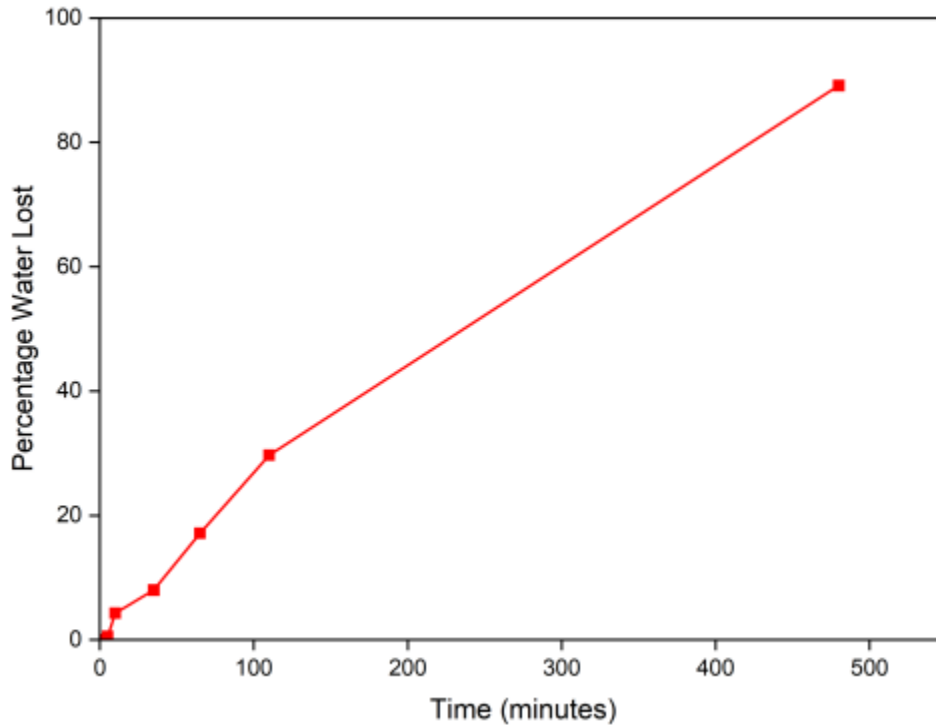
Figure 4.3. Percentage water lost by SAP when kept under sunlight with time at 35 ± 5 ℃ temperature.

4.2   Workability

In this study, the workability test was conducted, and the slump values of different GPC mixtures were measured, the results were depicted in Figure 4.4. It can be examined that the slump value varies from R0.5 to S0.554. The data showed that the mixture R0.554, which had a high ratio of AA/FA and without SAP, exhibited 20% increase in slump value compared to mixture R0.5. However, the results also revealed that the mixture S0.554, which contained SAP but had the same effective AA/FA ratio as R0.5, had almost identical workability to R0.5. By introducing extra alkali activator, the workability is improved.

This finding highlights the importance of maintaining an appropriate balance between AA and fly ash in GPC mixtures, as this can have a considerable influence on the final workability of the concrete. The workability of GPC mixtures decreases monotonically with SAP, and it was observed that the mixture S0.554 had a 14% lower slump value than R0.554, despite having the same total AA/FA ratio. This result was consistent with Fu et al. [111]. This phenomenon can be ascribed to the presence of SAP, which absorbs the alkali activator from the matrix initially, creating a less cohesive tissue in the matrix and, as a result, influences how slump values for various mixtures vary [83]. If no more alkali activator is added, a poorer workability is anticipated since SAP can absorb liquid from the activator and diminish the real AA/FA ratio. These effects would be mitigated by increasing the liquid content.
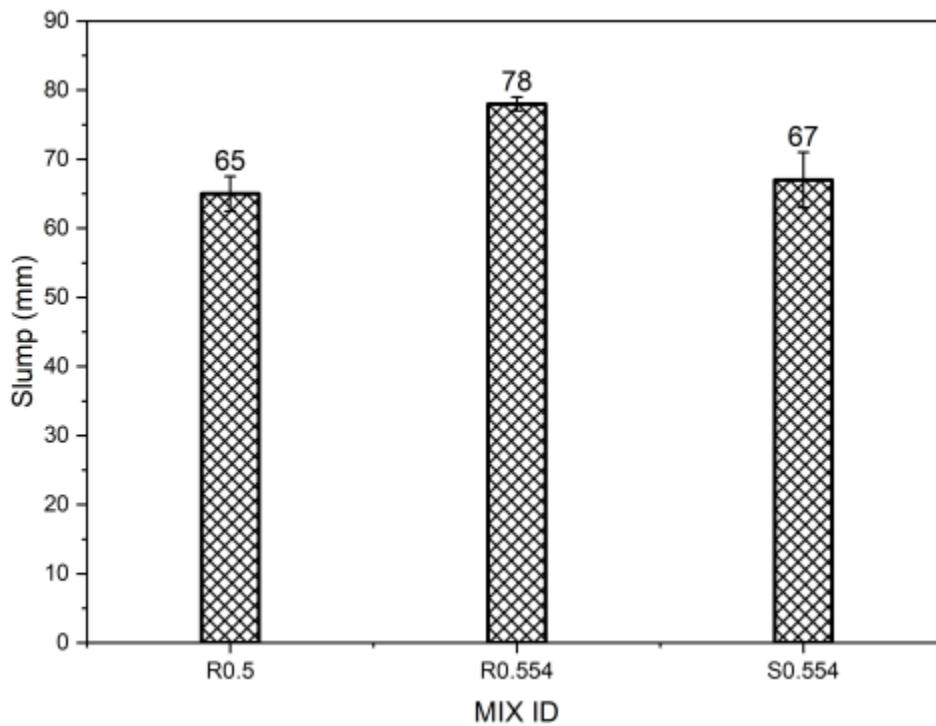
Figure 4.4. Slump values of GPCs.

4.3   Fresh and Harden Densities of GPC

This research has investigated the influence of SAP on the fresh and hardened densities of geopolymer concrete (GPC), and the findings are presented in Figure 4.5. It was discovered that the fresh density of GPCs expanded from 2425 to 2465 kg/m^3 with an increase in AA/FA ratio.

However, this trend was reversed when SAP was added to the mixture, causing the density to decrease to 2450 kg/m^3. The results also directed that the hardened densities of GPCs followed a similar trend, increasing with a rise in AA/FA ratio and decreases when SAP was added. In addition, it was observed that the mixture S0.554 had a lower density compared to R0.554 and a higher density compared to R0.5, whether in a fresh or hardened state.

The choice of AA/FA ratio and the inclusion of SAP can have a substantial effect on the final density of GPCs. Furthermore, it was noted that the hardened densities were lower than the fresh densities, which is due to water being thrust out as a result of geopolymerization [138]. Despite these fluctuations, the densities of the GPCs were found to be within the limits established by the ACI building code with densities of OPC concrete (2155 to 2560 kg/m^3) [139].
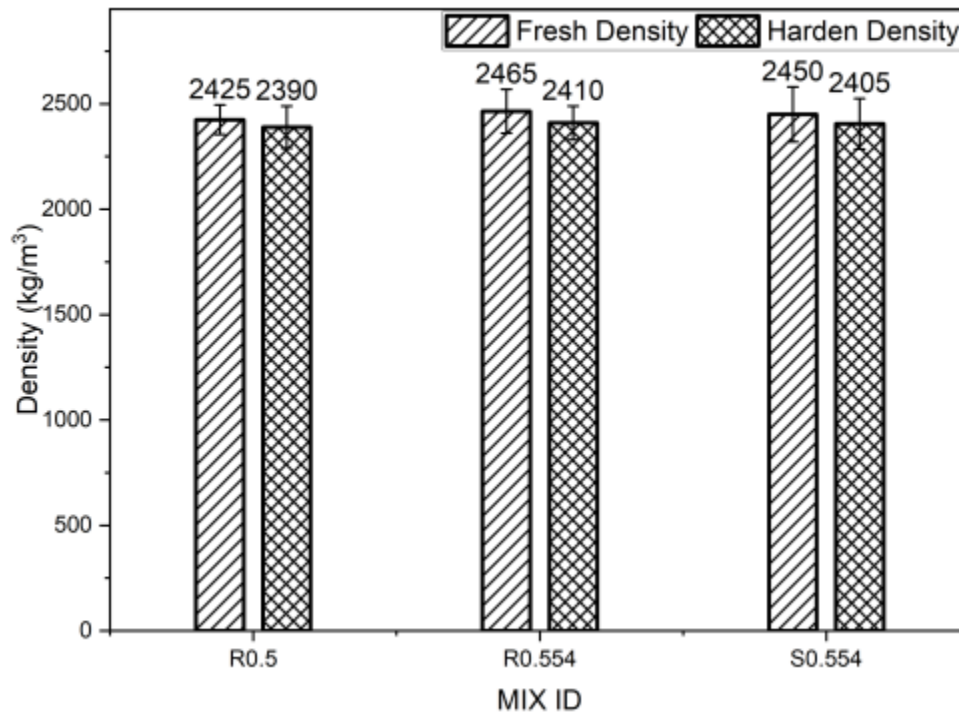
Figure 4.5. Effect of SAP on fresh and dry densities of GPCs.

4.4   Autogenous Shrinkage

The linear autogenous shrinkage of GPCs was assessed and the influence of SAP on autogenous shrinkage is represented in Figure 4.6. The results shows that a rise in the AA/FA ratio causes a 27% increase in autogenous shrinkage without SAP. The rationale is that by increasing the

amount of $[SiO_4]^{4-}$, the dissolution and reactivity of the binder might be accelerated, which will speed up the utilization of free water and improve the pore structure, leading to an increased capillary pressure [140]. However, IC by SAP can significantly reduce autogenous shrinkage, with the lowest amount of shrinkage observed in S0.554 and the highest in R0.554. It should be highlighted that the inclusion of SAP was successful in lowering the autogenous shrinkage.
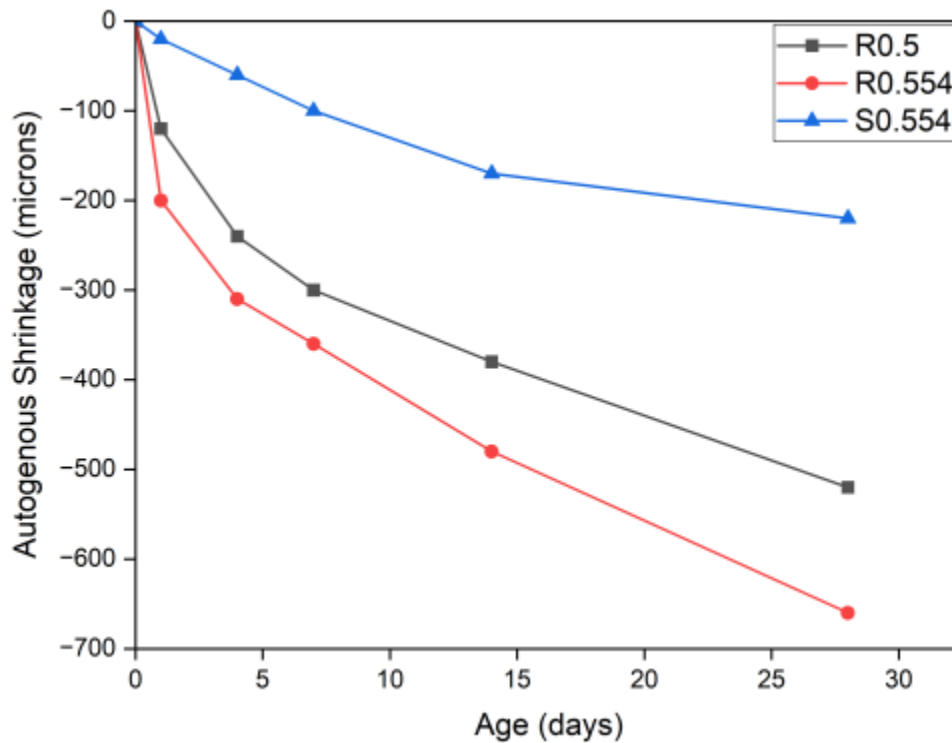
Figure 4.6. Effect of SAP on autogenous shrinkage of GPCs.

Interestingly, the addition of just 0.3% SAP to S0.554 caused a significant decrease in autogenous shrinkage when compared to R0.5. At 1, 7, 14, and 28 days, the reduction in autogenous shrinkage was approximately 83%, 66%, 55%, and 57%, respectively. Similarly, when comparing S0.554 to R0.554, the addition of SAP resulted in a reduction of autogenous shrinkage by about 90%, 72%, 64%, and 66% at 1, 7, 14, and 28 days, respectively. This outcome is comparable to the alkali-activated fly ash/slag mortar's autogenous shrinkage in earlier studies by Jiang et al. [88], J. Yang et al. [92]. It is significant to observe that autogenous shrinkage of the pastes is produced by capillary forces, which in turn are brought on by the drop in RH that was explained by [87]. However, the researchers [109] found that SAP releases alkali activator into the paste, maintaining RH and reducing self-desiccation, rather than causing expansive crystal growth or the development

43

of a denser microstructure with less deformability. Overall, the findings suggest that SAP curing leads to an elevated RH, which effectively reduces self-desiccation and ultimately decreases autogenous shrinkage.

4.5   Total Drying Shrinkage

The total drying shrinkage has been measured and evaluated with the addition of SAP. The outcome of this study is illustrated in Figure 4.7. The autogenous shrinkage is also a part of total drying shrinkage, so both the shrinkages graphs followed a similar pattern. The results of the study revealed that R0.554 exhibited the maximum total drying shrinkage. However, on the other hand, S0.554 manifested the minimum total drying shrinkage. Upon an increase in the AA solution, the reference specimens demonstrated an increase in total drying shrinkage. The inclusion of SAP was observed to reduce the total drying shrinkage of GPC by an impressive margin of 60% to 80%, as compared to both reference specimens.
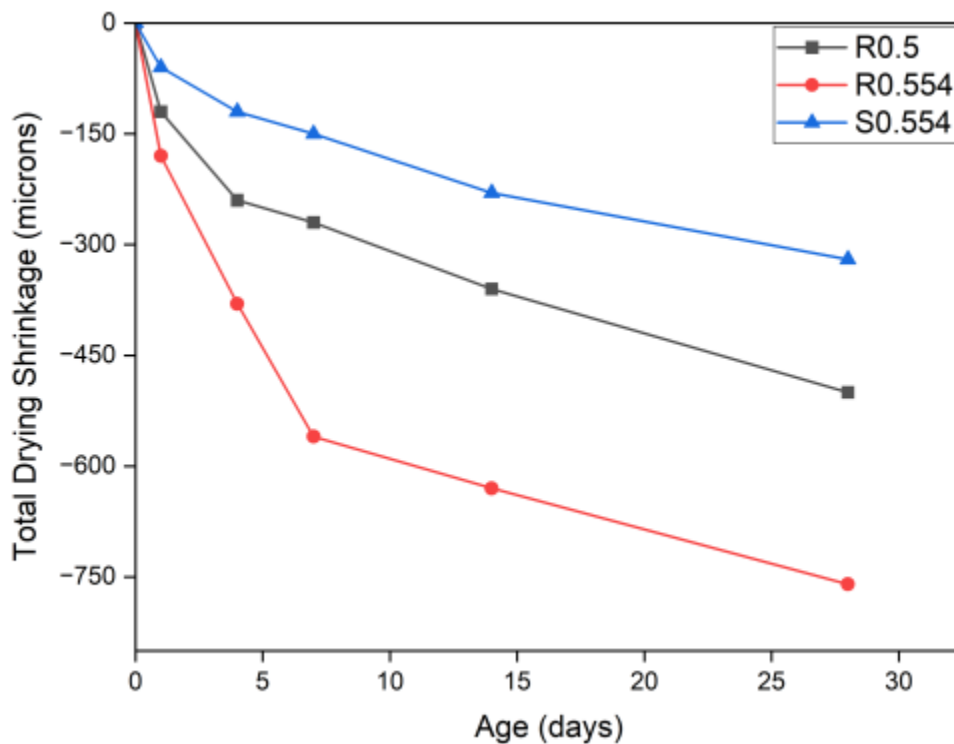
Figure 4.7. Effect of SAP on total drying shrinkage of GPCs.

This outcome is a clear indication that SAP plays an essential role in mitigating the total drying shrinkage of GPC. Incredibly, the addition of only 0.3% SAP concentration was found to eliminate

approximately 58% and 36% of the total drying shrinkage when compared to R0.554 and R0.5, respectively. The impact of SAP on total drying shrinkage was found to be consistent with its effect on autogenous shrinkage explained in section 4.4. The study's outcomes indicate that the substantial reduction in autogenous shrinkage observed due to the presence of SAP was the cause of the reduction in total drying shrinkage. The findings of this study are in good agreement with previous researches by Ma et al. [99] and Fu et al. [111].

4.6   Mechanical Properties

4.6.1. Compressive Strength

The compressive strength of concrete is one of the most important properties used to assess its quality and performance. The experiment involving the compression test was conducted on all the mixes, and the outcomes of the GPC compressive strength test at 28 days were exhibited in Figure 4.8, which displayed a significant increase in the compressive strength of GPC with an increase in AA/FA ratio without SAP, which was also reported by Ghafoor et al. [120]. However, the introduction of SAP into the mix had an unfavourable effect on the compressive strength of the GPC, at an equal total AA/FA ratio. The compressive strength of the GPC mix S0.554 decreased by 2%, 5%, and 7% compared to R0.554 at the water, ambient, and heat curing, respectively, when the total AA/FA ratio was kept constant due to the voids induced by SAP [110], which was proved in section 4.13. The dilution of alkalis in pore solution, which lowers pH and slows the binder dissolution, is another potential cause of the strength drop in SAP-cured AAS [111]. The strength loss increases as the amount of SAP added increases [111]. Effective AA/FA ratio representing the available amount of free activator during mixing. It was observed that the presence of more activators in the mix compensated for the negative effect of SAP, and the compressive strength increased when the effective AA/FA ratio was kept constant.

Usually, liquid within the enlarged SAP participates in additional chemical reactions. The water and activators released continuously by SAP during the IC process played a crucial role in enhancing the N-A-S-H/C-A-S-H gel content by promoting the polymerization reaction [112]. This improvement in the mechanical properties of the AAS pastes was also attributed to the development of an interfacial transition zone around the SAP void. The slower activator release from larger SAP particles can progressively enhance the geopolymerization around the particles

and make up for the compressive strength loss brought on by the development of macropores. This zone helped reduce the size of the SAP-induced micropores and pore volume investigated by J. Yang et al. [112]. However, among the other external curing methods, heat cured specimens showed the better compressive strength and water cured samples have the minimum compressive strength. When compared to ambiently cured specimens without SAP for R0.5-A, heat-cured specimens R0.5-H had a 34% higher compressive strength, but when SAP was introduced in S0.554-H, the increase in compressive strength dropped to 26% compared to S0.554-A having similar total AA/FA ratio to GPC specimens. The performance of S0.554 was found to be the best at ambient curing, with a 7% improvement in strength, while for water curing and heat curing only 3% and 1% increase in compressive strength was observed compared to R0.5, respectively. In heat curing, most of the hydration took place during the heating period, So SAP was found less effective due to the loss of the activator during the first day of curing.
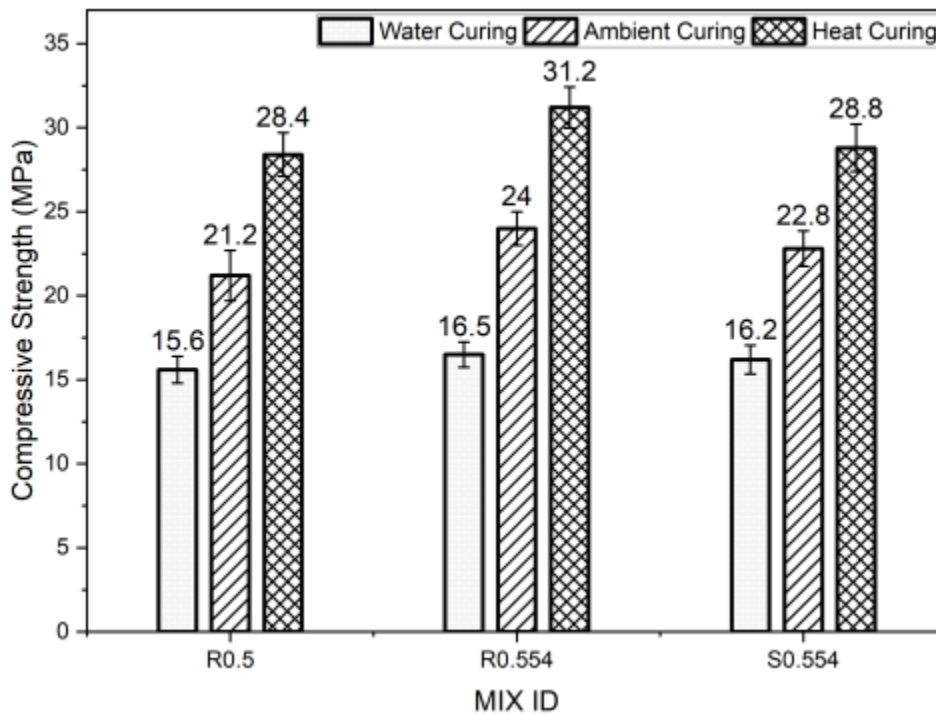

Figure 4.8. Effect of SAP on compressive strength of GPCs after 28 days in different curing conditions.

4.6.2. Flexural Strength

The results of the flexural strength test conducted on GPCs and the effects of SAP on the Modulus of Rupture under different curing conditions are illustrated in Figure 4.9. It was found that the flexural strength of GPCs increases with an increase in the AA/FA ratio, a phenomenon previously described by Ghafoor et al. [120], for samples without SAP. This is consistent with the compressive strength described in sections 0, which showed that higher AA/FA ratios lead to stronger specimens. However, the addition of SAP improved the flexural strength of the GPCs as well. The positive effect of SAP was particularly pronounced when compared to reference specimens R0.5 that had a similar effective AA/FA ratio, with 6% to 18% improvement in flexural strength. Despite the various external curing methods used, heat curing exhibited the highest flexural strength while water curing yielded the lowest. The flexural strength of heat-cured specimens was 18% greater than that of ambient-cured specimens without SAP containing AA/FA ratio 0.5, but this difference decreased to 7% for S0.554-H compared S0.554-A, when SAP was added at similar total AA/FA ratios to GPC specimens.

The increase in flexural strength was attributed to the reduction in autogenous shrinkage caused by SAP. This reduction, in turn, reduced the development of microcracking at an early age and ultimately led to an improvement in flexural strength [109]. Contrary to compressive strength, flexural strength determined by three-point bending is extremely susceptible to microcracking. The un-hydrated precursor particles, such as fly ash having crystalline segments, might locally constrain the shrinkage of gel bordering them and cause microcracking [141], even though the samples for strength tests were not under externally restrained conditions during curing. Although the samples were exposed for less than 60 minutes before being tested, more shrinkage may result from drying the sample when it is visible to the conditions (RH of 50%) during a strength test.

It was observed that the influence of the addition of SAP was more significant in ambient curing and least effective in heat curing. In ambient curing, the incorporation of SAP led to a remarkable 18% and 13% improvement for S0.554-A compared to R0.5-A and R0.554-A at similar effective and total AA/FA ratios, respectively. Whereas in case of heat curing, the minimal improvement of 6% and 4% was observed for S0.554-H compared to R0.5-H and R0.554-H, respectively. In water curing, the results were also noticeable, with a 12% and 8% increase in flexural strength for SAP-modified samples compared R0.5-W and R0554-W, respectively. The incorporation of SAP has

not only improved the overall strength of the GPCs but has also made them more resilient to damage and cracking.
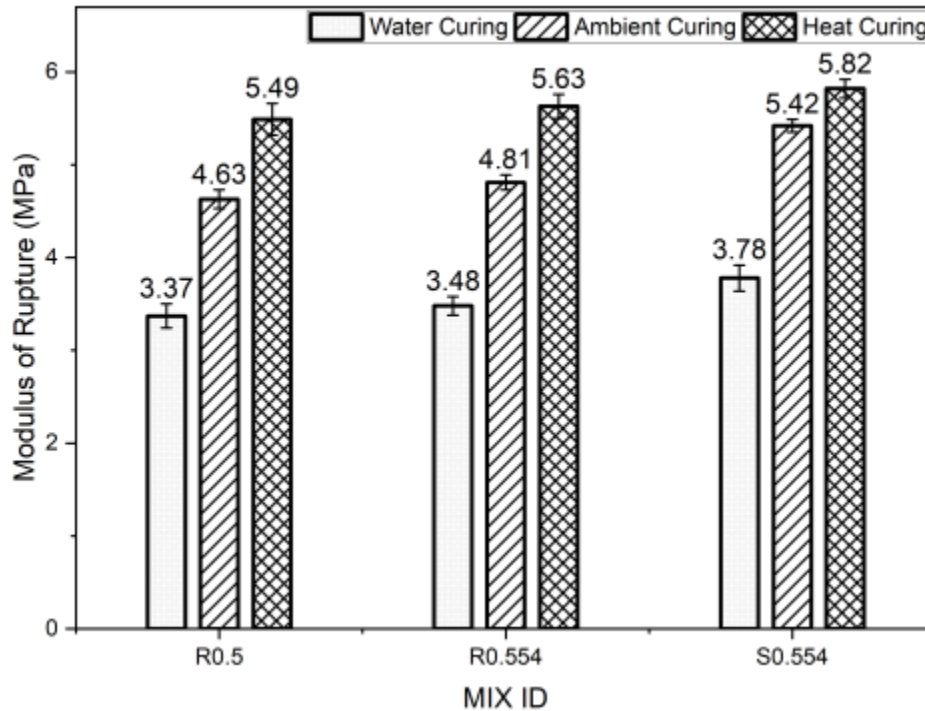
Figure 4.9. Effect of SAP on flexural strength of GPCs after 28 days in different curing conditions.

4.6.3. Tensile Strength

The tensile strength test of GPCs was performed as per ASTM C496 [130] and the outcomes of which are demonstrated in Figure 4.10. The results show that the tensile strength of GPCs was notably enhanced by the addition of SAP, much like the improvement seen in the flexural strength test described in section 0. The superior performance of SAP was observed in the case of ambient curing, while this performance enhancement was minimal in case of heat curing specimen. The addition of SAP resulted in a significant improvement in tensile strength in ambient curing for S0.554, with a 35% and 15% increase observed compared to R0.5-A and R0.554-A at similar effective and total AA/FA ratios, respectively. In the case of heat curing, the increase was 11% and 2%, and for water curing, the increase was 21% and 2% compared to R0.5-H and R0.554-H.

Heat-cured specimens exhibited the highest tensile strength among the external curing technqiues, while water-cured samples had the lowest. In comparison to ambient-cured specimens R0.5-A lacking SAP, heat-cured specimens R0.5-H showed a 43% increase in tensile strength, but the enhancement decreased to 17% when SAP was included (S0.554-H compared to S0.554-A), resulting at similar total AA/FA ratios to GPC specimens. This showed that incorporation of SAP was found most effective with ambient curing conditions. According to Eurocode 2, tensile strength and flexural strength are directly proportional to each other [142], and these findings concur with those of the flexural strength test as well described in section 4.6.2. Flexural Strength. This enhancement in tensile strength can be attributed to the reduction in autogenous shrinkage and the development of microcracking, leading to an overall improvement in the mechanical properties of GPCs.
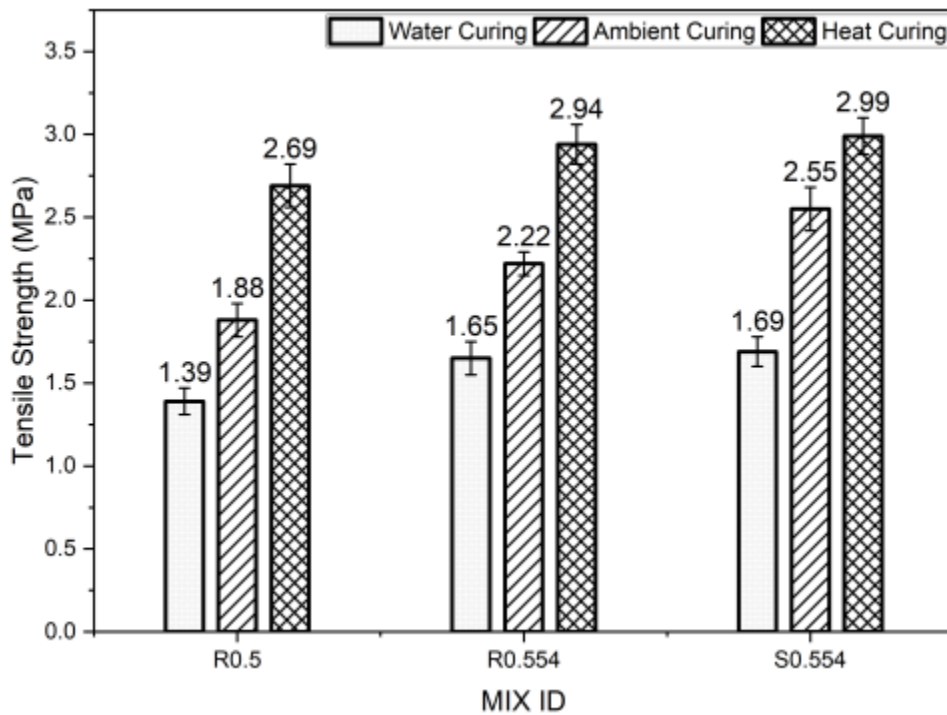
Figure 4.10. Effect of SAP on tensile strength of GPCs after 28 days in different curing conditions.

4.7   Strength Development in GPCs

The strength development of GPCs was closely examined, and the results are presented in Figure 4.11. The results clearly show that the action brought on by the SAP increased the strength growth at a later age. However, the addition of SAP to the specimens had a negative impact on the early age strength. It was found that the strength deficit produced by the voids originated by SAP could be equal to or even higher than the strength gain produced by the IC action [86]. According to previous research by Hasholt et al. and D. Snoeck et al. excess water absorption by SAP can have both early and later impacts on the strength development of cementitious materials [143], [144]. It was also discovered that greater amounts of SAP are expected to have both beneficial and detrimental effects in cementitious materials with low water-to-binder ratios. However, lower amounts of SAP may have a more noticeable positive impact. In summary, the results of this study demonstrate that the IC action induced by SAP can enhance the strength growth of GPCs, but it's essential to carefully balance the amount of SAP added to avoid negative impacts on early-age strength.
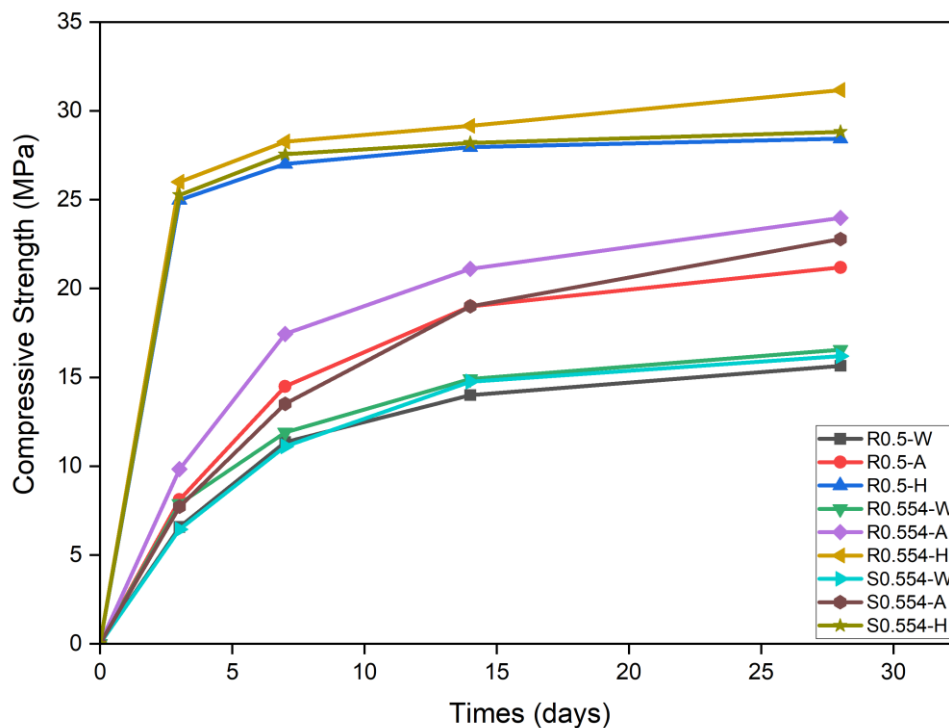
Figure 4.11. Effect of SAP on compressive strength development of GPCs in different curing conditions.

4.8 Bulk Resistivity

The Bulk Resistivity test on GPCs at 28 days showed that the addition of SAP and an increase in the AA/FA ratio reduced the value of bulk resistivity, as demonstrated in Figure 4.12. Resistivity values for S0.554 were significantly lower than those for R0.5, but higher than those for R0.554. The addition of SAP for S0.554 decreased the bulk resistivity by 1% for all curing types when compared to R0.5 at similar effective AA/FA ratios but increased by 5% for ambient curing, 4% for heat curing, and 2% for water curing at similar total AA/FA ratios compared to R0.554. Similar like mechanical strength test results, heat curing produced specimens with the least electrical resistivity among other external curing methods, whereas water curing resulted in the highest. The compressive strength data as discussed in section 0 also followed a similar trend which showed that R0.554 will have a more compact pore structure at older ages than R0.5. Vafaei et al. have demonstrated that an increase in the total AA/FA ratio led to a decrease in electrical resistivity in pastes containing SAP [87].
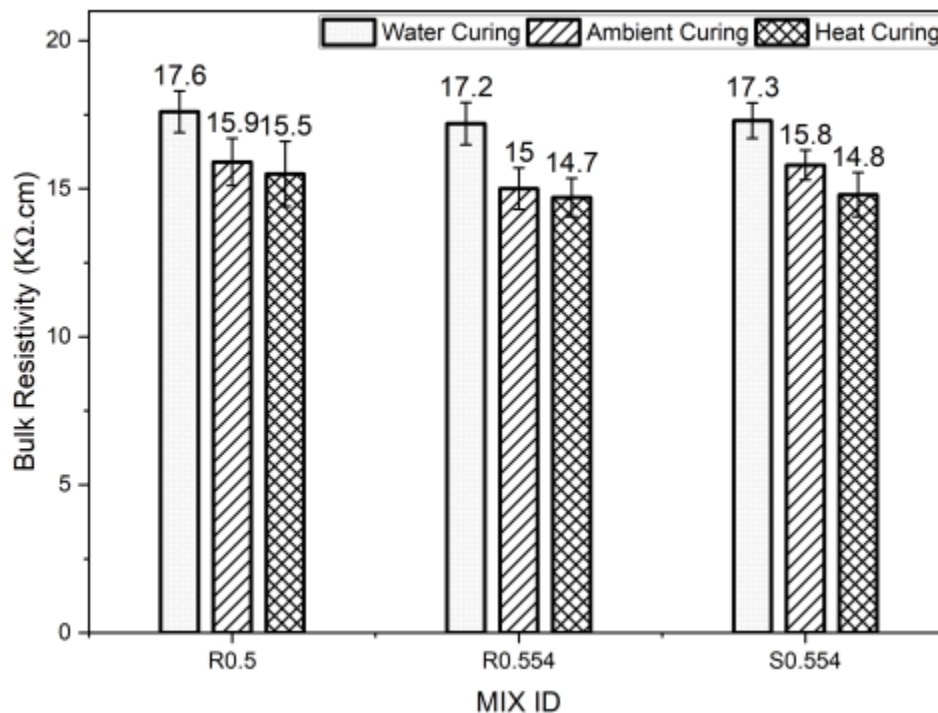
Figure 4.12. Effect of SAP on bulk resistivity of GPCs after 28 days in different curing conditions.

4.9   Ultrasonic Pulse Velocity

The ultrasonic pulse velocity (UPV) test was carried out in this study on GPCs. In Figure 4.13, the results of the ultrasonic pulse velocity (UPV) test on GPCs with and without SAP are presented. The data indicate that the addition of SAP to GPCs improved their quality and resulted in higher UPV values, which is an indicator of uniformity and good quality in concrete [114]. In addition to SAP, increasing the AA/FA ratio also improved the quality and increased UPV. Among all the specimens, R0.554-H exhibited the highest UPV value when heat cured. While other external curing methods produced different results, heat curing resulted in the highest UPV value, while water curing yielded the lowest value of UPV.
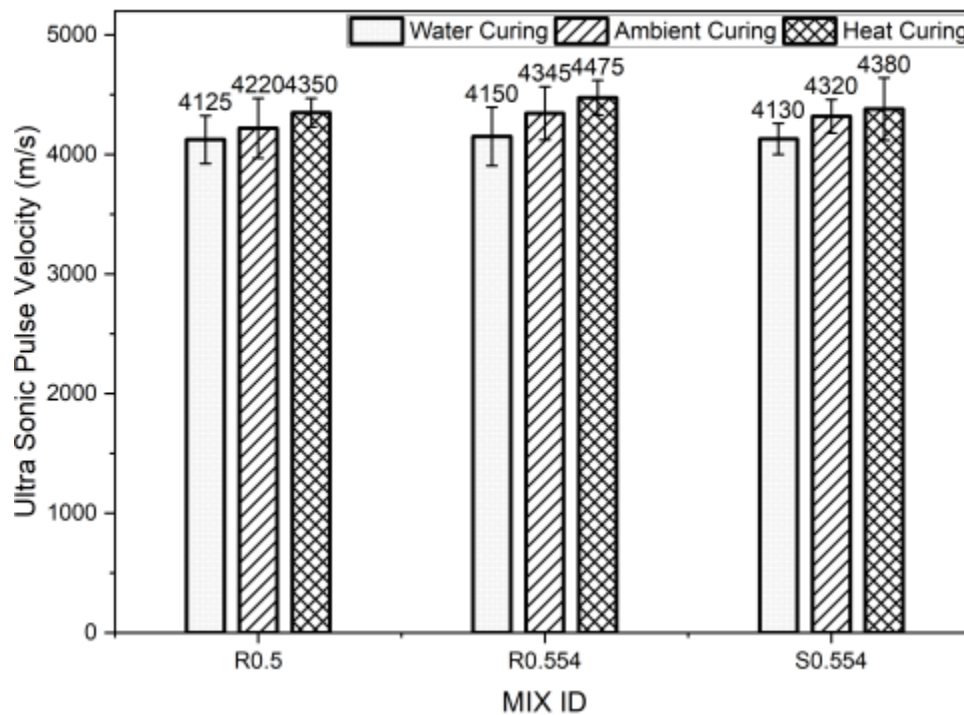
Figure 4.13. Effect of SAP on ultra-sonic pulse velocity of GPCs after 28 days in different curing conditions.

Heat-cured specimens R0.5-H showed a 3% greater UPV value compared to ambient-cured specimens R0.5-A without SAP but it decreased to only 1% when SAP was added in S0.554-H compared to S0.554-A at similar total AA/FA ratios to GPC specimens. The UPV results were consistent with the mechanical strength results of section 4.6 and bulk resistivity test results from

section 4.8, showing a correlation between higher UPV values and increased strength. Notably, SAP was most effective in ambient curing conditions, demonstrating the importance of proper curing conditions in optimizing the benefits of SAP in GPCs.

4.10   Permeability

Figure 4.14 showcases the results of the permeability test on GPCs. The specimens were split along the middle after applying pressure and the maximum depth of water penetration was measured. The findings demonstrate that the inclusion of SAP significantly reduces the permeability of GPCs, which translates to a major improvement in the quality of concrete as discussed earlier in section 4.6. This reduction in permeability is due to the modifying effect of SAP on the pore structure of the concrete matrix. As reported by Z. Yang et al., when SAP is added to the mixture, a considerable amount of liquid is absorbed by the SAP particles [93]. This leads to a reduction in the available liquid in the interstitial space and, as a result, a lower effective liquid-binder ratio. Different external curing methods yielded varying results, with heat curing producing mixes R0.5-H, R0.554-H and S0.554-H the least penetration depth of water was found and water curing resulting in the maximum value of permeability values for R0.5-W, R0.554-W and S0.554-W samples.

Z. Yang et al. studied that the pores captured by SAP are known as ink bottle pores and are far less interconnected than capillary pores present in the binders [93]. In addition, the volume of SAP increases after grasping water, which restricts the movement of water within the specimen, as a result, a higher permeability pressure is needed to permeate the mixtures containing SAP. It should be noted that while the addition of SAP enhances the impermeability of GPCs, excessive amounts of SAP can have an adverse impact on permeability. If the proportion of SAP exceeds a certain threshold, it results in an increase in manually added pores, which can weaken the concrete matrix [93]. Additionally, excessive water release can lead to an increase in porosity, creating more linked pores and accelerating the passage of free water. The findings of this study confirm that the addition of SAP can improve the impermeability of GPCs, which can have significant implications for the durability and longevity of concrete structures.
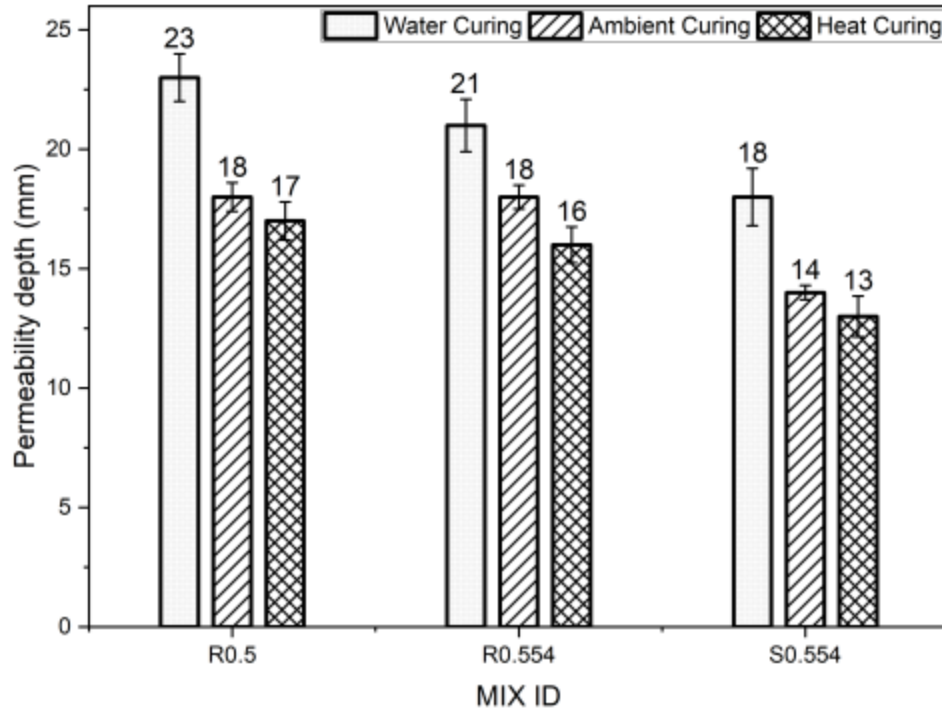
Figure 4.14. Effect of SAP on permeability depth of GPCs after 28 days in different curing conditions.

4.11 Water absorption and volume of permeable voids (VPV)

The water absorption and volume of permeable voids in GPC were determined. Figure 4.15 illustrates the effect of SAP on water absorption, indicating a notable decrease in absorption, which is consistent with the results obtained from the permeability tests from section 4.10. The inclusion of SAP produced a significant enhancement in all curing methods, including a reduction in the water absorption of GPCs. Specifically, in ambient curing, there was a substantial decrease of 28% and 22% in water absorption for S0.554-A was found when compared to reference mix R0.5-A and R0.554-A at similar effective and total AA/FA ratios, respectively. Similarly, S0.554-H and S0.554-W exhibited noticeable decreases, with a 4% and 6% decrease at the same effective AA/FA ratio compared to reference mix R0.5-H and R0.5-W, and a 2% and 5% decrease at the same total AA/FA ratio compared to reference mix R0.554-H and R0.554-W, respectively.

Similarly, the effect of SAP on the number of permeable voids is revealed in Figure 4.16, which shows a clear decrease in the number of such voids with the addition of SAP. In all curing types,

the addition of SAP resulted in significant improvement, with a 15% and 7% decrease in the volume of permeable voids by S0.554-A compared to R0.5-A and R0.554-A at similar effective and total AA/FA ratios, respectively. Both heat curing and water curing exhibited significant reductions, with a 13% decrease for S0.554-H and a 6% decrease for S0.554-W, at the equivalent effective AA/FA ratio compared to reference specimens R0.5-H and R0.5-W, respectively. Moreover, at the same total AA/FA ratio, permeable voids experienced a 13% decrease for S0.554-H and a 9% decrease for S0.554-W compared to R0.554-H and R0.554-W, respectively. Heat curing produced specimens with the lowest water absorption and volume of permeability voids among other external curing methods, whereas water curing resulted in the lowest. The water absorption and volume of permeability voids of heat-cured specimens R0.5-H were 16% and 6% lesser than that of ambient-cured specimens R0.5-A without SAP, and this difference decreased to 11% and 4% for the mix S0.554-H when SAP was added compared to S0.554-A, with similar total AA/FA ratios as GPC specimens.
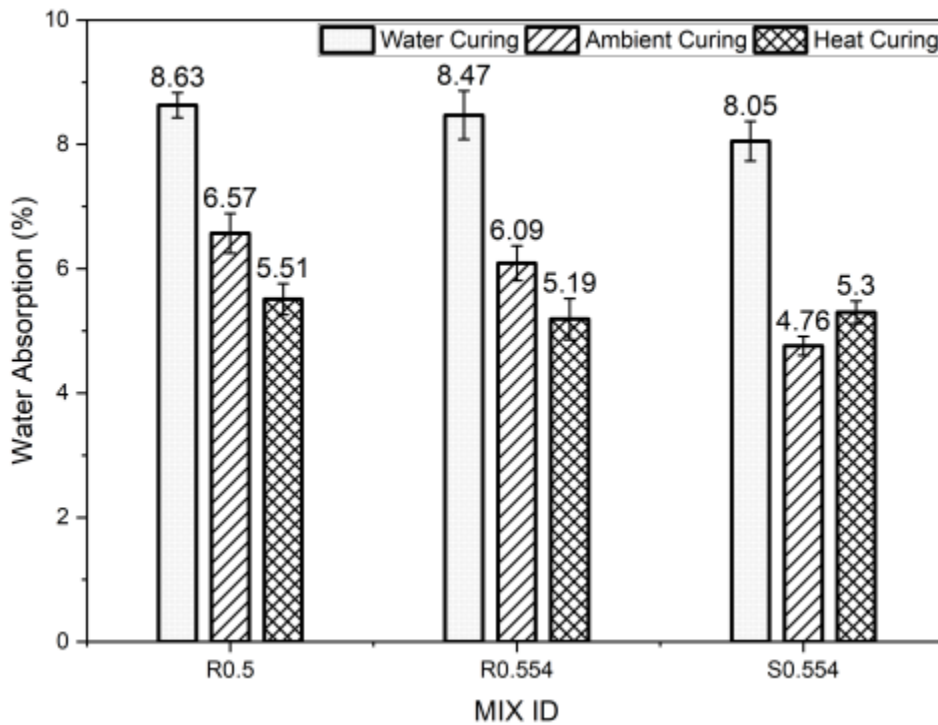
Figure 4.15. Effect of SAP on water absorption of GPCs after 28 days in different curing conditions.

It is important to note that the lower absorption observed with the addition of SAP is indicative of a reduction in surface porosity, which is a key factor in determining the degree of water penetration in GPCs [145]. Therefore, the use of SAP particles in GPCs is highly beneficial in reducing water permeability and surface porosity, thereby resulting in concrete structures that are highly durable and resistant to water damage. These findings demonstrate the great potential of SAP in enhancing the long-term durability and performance of GPCs in various applications.

The early-age stage of mixing and curing is when the OPC or alkali activated matrix consumes the most liquid to create hydration products. Thus, the presence of liquid inside the matrix with enlarged SAPs caused the rate of porosity reduction raised. Since the SAPs had a lot of water in them, the matrix's porosity decreased as a result, and this process continued over the course of the 28 days [86]. Similarly, Jiang et al. and Z. Yang et al. explained that more gel holes are present in the SAP-modified sample than in the reference sample [88], [91].
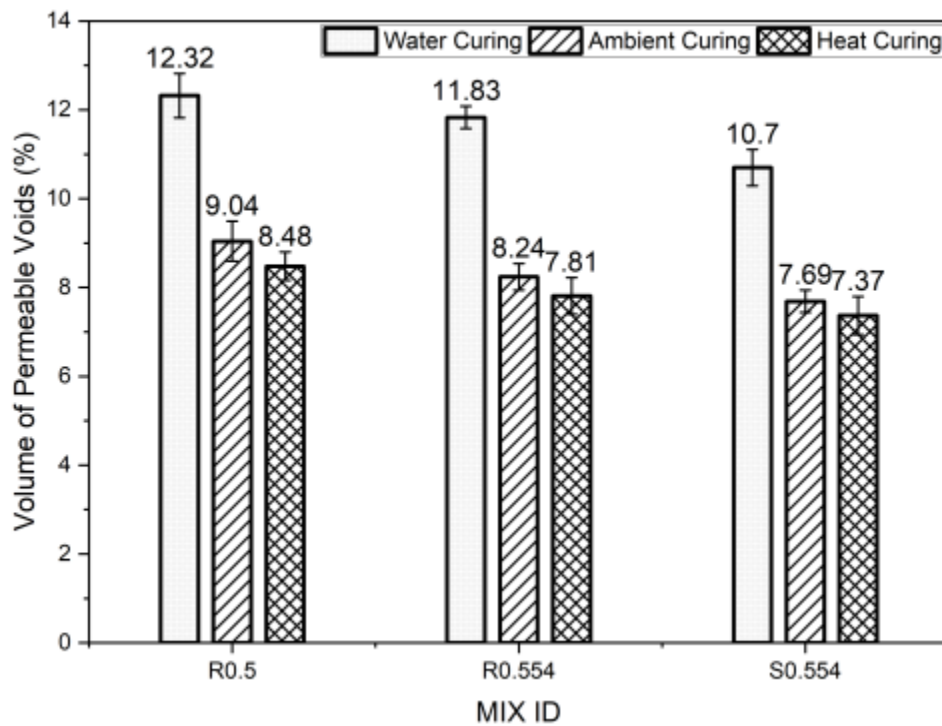
Figure 4.16. Effect of SAP on volume of permeable voids of GPCs after 28 days in different curing conditions.

For this reason, internal curing by SAP may encourage the hydration of binders, produce more N-A-S-H / C-A-S-H gels, and consequently increase the content of gel pores. Accordingly, to Jiang et al. the capillary pore structure of the nearby alkali activated pastes changed the number of capillary pores in the SAP-modified specimens as compared to the reference [88]. The cause may be that, with the exception of the empty space entrusted by SAPs themselves after discharging water, internal curing water and activators would seep into the alkali activated pastes and eventually create capillary pores.

4.12 X-ray Diffraction (XRD)

X-ray diffraction of finely grinded paste obtained from GPCs was carried out and the XRD patterns are displayed in Figure 4.17. The identification of different phases in GPCs was made possible through the use of XRD, which demonstrated the geopolymerization activity. The X-ray diffractograms of geopolymer samples reported the creation of mullite ($3Al_2O_3 2SiO_2$ or $2Al_2O_3 SiO_2$) and sodalite ($Na_8(Al_6Si_6O_{24}) Cl_2$) [94].
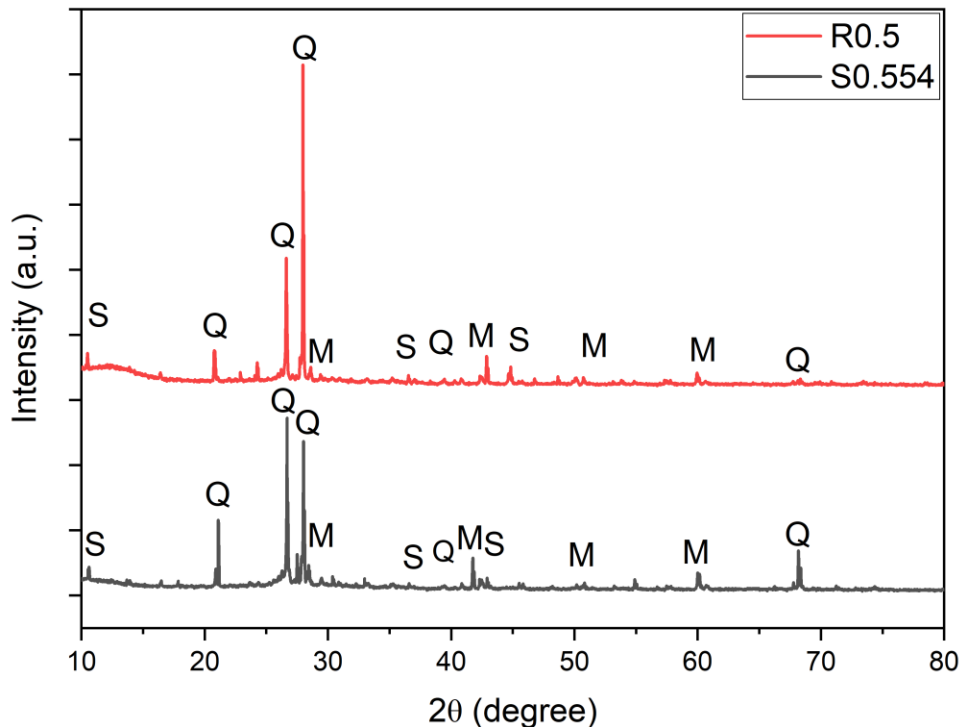
Figure 4.17. XRD patterns of R0.5 and S0.554 ambient cured for 28 days. M, S, and Q indicate Mullite ($3Al_2O_3 2SiO_2$ or $2Al_2O_3 SiO_2$), Sodalite ($Na_8 (Al_6Si_6O_{24}) Cl_2$), and Quartz ($SiO_2$), respectively.

The sharp peaks of Sodalite and Mullite in R0.5 indicated that the SiO_2 and Al_2O_3 of the fly ash were not totally utilized in the geopolymerization reaction [146]. The sharpness of the mullite and sodalite-related peaks was observed to be lower for S0.554 than for R0.5, indicating that the IC technique promoted the geopolymerization reaction of GPCs. The inclusion of SAP only caused a less sharp peak of the main hump but did not produce new types of reaction products. This is most likely because the liquid produced from SAP made it easier for fly ash to react further, producing more products as well as slightly different products from the original hydration products that was also noticed by Z. Yang et al. [93]. The findings demonstrate that the addition of SAP to GPCs could enhance their geopolymerization activity and promote the development of desired reaction products.

4.13   SEM

The small chunks from GPC specimens with and without SAP were analysed through SEM examination as seen in Figure 4.18, the microscopic photographs showed the cracked surface of GPCs after 28 days of ambient curing. The images contain a few microcracks that could be due to shrinkage that happened during sample preparation or curing [147]. The primary cause of the dense microstructure is that the activator offers nuclei (such as silicates) for the evolution of reaction products in the interstitial place in addition to a high pH environment for the dissolving of fly ash [148]. It is evident that the GPC matrix is dense and without large capillary voids, and that reaction products have covered the fracture surface. The matrix has embedded and randomly distributed SAP particle vacancies. It was noticed that there were small, unrecognized crystals scattered throughout the matrix. However, the S0.554 microstructure showed a denser and more dense microstructure, with several phases in a better-distributed state compared to R0.5, which is consistent with the results of Afridi et al. [94]. The unreacted reactants were observed in R0.5, while the S0.554 microstructure showed that geopolymerization had occurred to a larger extent, leading to a denser and more compact structure.

Furthermore, SEM images of GPCs containing SAP showed a denser and flocculated fabric made of SAP-geopolymeric gel, with the matrix having embedded and randomly distributed SAP particle vacancies. The void generated from SAP was depicted in Figure 4.19, which was expected from the form of dry SAP particles. No dry SAP particle was discovered in the void, most likely because polishing process eliminated it. It's also important to note that a light grey layer develops

between the SAP void and the GPC matrix. The internal curing activators and water discharged from SAP encourage the reaction of fly ash, and that once some deliquescent Na^{2+}, Al^{3+}, and $[SiO4]^{4-}$ distributed from pore solution to SAP cavity, an ITZ eventually forms around SAP cavity [88]. These spaces confirmed that SAP significantly absorbed the liquid and expanded during mixing, as explained by Z. Yang et al. [93]. In summary, the SEM examination discovered that the inclusion of SAP caused a denser and more compact microstructure with embedded SAP particles, which could have positive implications for the strength and durability of the GPCs.
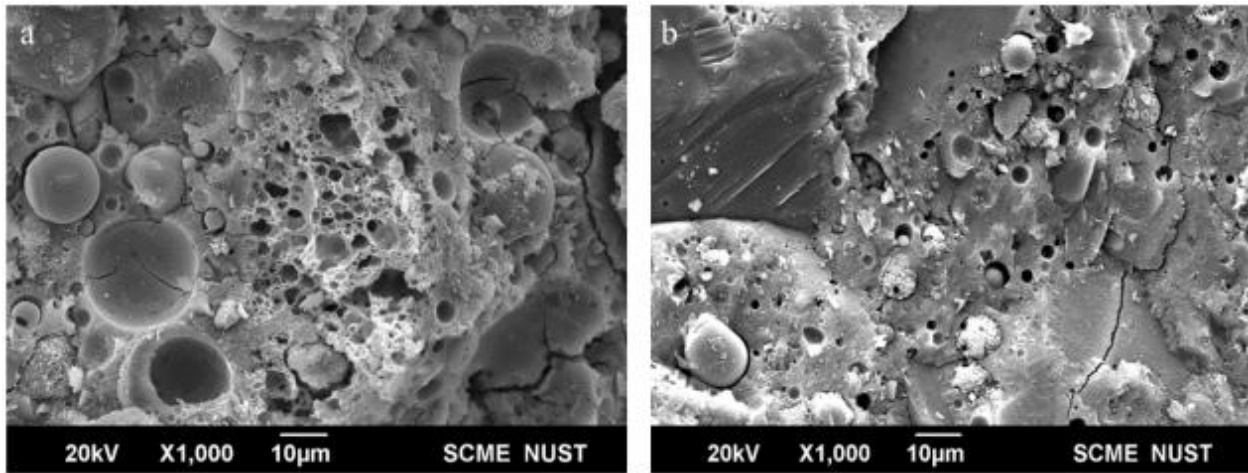
Figure 4.18. SEM images of (a) R0.554 and (b) S0.554 ambient cured for 28 days.
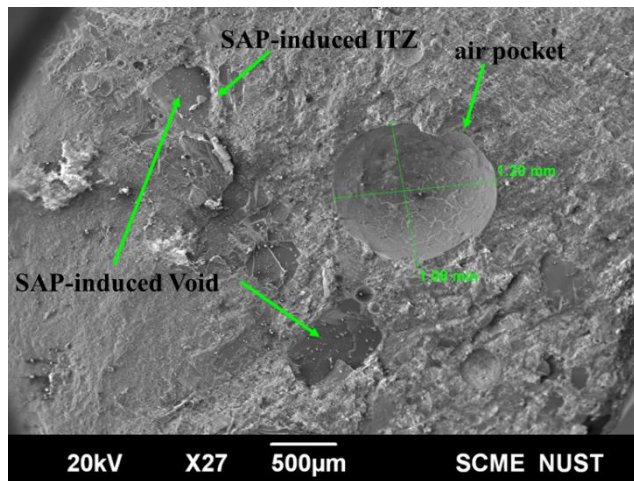
Figure 4.19. SEM image of SAP induced void.

Chapter 5

5. Discussion

The ions present in the activator causes of the SAP absorption capacity in the GPC supernatant being only 17% of that in tap water. As the density of the anionic groups in solution of $Ca(OH)_2$ increases, it has been observed that SAP's ability to absorb liquid gradually declines [73]. Additionally, the electronic barrier effect caused by the existence of multi-ions in the mix alters the reaction forces among molecules in SAP polymer chains. Cross-linking of molecular chains can be brought on, particularly by Ca^{2+} and Al^{3+} [73].

The differential in ion concentration between internal and exterior surroundings also affects how well SAP absorbed the liquid [149]. The osmotic pressure would be smaller and SAP's absorption capacity would be decreased since the activator has large ion concentrations. Jensen & Hansen explained that the range of ions in the cement slurry and the elevated ionic concentrations of the solution are the two major causes of the variance in SAP's absorption capacity in different solutions [72].

The S0.554 experienced the least autogenous shrinkage, whereas the R0.554 experienced the most. This is due to the fact that early ages of alkali activators' quick reaction in binders resulted in a large number of mesopores that were smaller than the pores in the SAP-modified mixture, resulting in an increase in capillary tensile force and consequently an increased shrinkage [150], [151]. In other words, the specimens with the largest drop in internal RH shown more autogenous shrinkage.

Since the loss of moisture can be supplied and the distortion brought on by self-desiccation and the volume drop of chemical reactants can be controlled by SAP, the inclusion of SAP as an IC agent in the alkali activated systems can effectively limit autogenous shrinkage [83]. Additionally, the released activator refines capillary pores, which lessens the power behind autogenous shrinking because the enlarged SAPs provided all the liquid needed for the hydration process.

The inclusion of SAP particles reduces the drying shrinkage as well, along with autogenous shrinkage. According to the fundamentals of capillary pressure theory, the Kelvin radius and pore size distribution perform a major role in determining the quantity of moisture loss in alkali activated systems under a specific drying RH [152], [153]. The meniscus radius in capillary pores,

known as the Kelvin radius, is mainly determined by the water activity and RH of the pore solution. Since the same RH was used to dry all alkali activated specimens with varying SAP inclusion, the Kelvin radius is consistent across all systems.

As a result, the pore structure of alkali activated systems has a substantial impact on the behaviours of early age drying shrinkage. Since the moisture from the pores and voids formed by the SAP is preferably dissipated under the same drying RH, the mass loss is increased in alkali activated systems with the incorporation of SAP. As a result, the water emitted from the SAP delays the drop in internal RH, which reduces the early stages drying shrinkage [111].

Heat curing was best among all external curing due to the increased rate of geopolymerization reaction at higher temperatures. These results are consistent with the findings of Poloju & Srinivasu [154], whereas water curing was the least effective curing method for GPC in all cases because the source of activation, which consisted of alkali activator, caused a significant issue in the overall quality of the specimens. When immersed in water, the alkali activator salts were leached out of the pores, causing an increase in water absorption as described by El-Feky et al. [27].

As the curing time increased, a higher amount of NaOH solution was pushed out of the pores. This process led to the partial prevention of the geo-polymerization reaction, ultimately resulting in lower amounts of geopolymer gels being created [27]. As a result, the specimens became more porous, decreasing their overall quality. Ambient curing of GPC can produce improved strength over water curing as discussed in section 3.6, which was also observed by Abdalqader et al. [35]. Similarly, Mayhoub et al. explained that the process of geopolymerization in GPC does not include water [155]. As a result, the GPC matrix is less compacted and has more voids. This could account for why the compressive strength of the water-cured specimen decreased.

The SAP-modified specimens showed better physical, mechanical and microstructural properties compared to the reference specimens for all external curing methods. The liquid contained in the SAP typically undergoes additional chemical reactions. The continuous release of water and activators by SAP during the IC process has a vital role in promoting the geopolymerization reaction and increasing the content of N-A-S-H/C-A-S-H gel, which was also verified in section X-ray Diffraction (XRD) and SEM.

The enhancement of these properties in AAS pastes is also attributed to the formation of an interfacial transition zone surrounding the voids created by SAP that can be seen from Figure 4.19. The slower release of activators from larger SAP particles gradually improves the geopolymerization process around the particles, as debated in section Mechanical Properties. This zone helps reduce the size of micropores induced by SAP and pore volume, as investigated by J. Yang et al. [112].

It is well known that fly ash-based GPC needs to be heated to reach the necessary early mechanical strength properties, which could be a major obstacle for on-site applications [156]. Compared to GPC cured at ambient temperatures, GPC cured at higher temperatures showed a more noticeable increase in mechanical strength [157]. This is because greater temperature curing results in earlier polymerization than open air does [154]. Microstructural analysis of the impact of heat curing on fly-ash based GPC was performed by Abdollahnejad et al. [158] and the findings demonstrated that thermal treatment leads in denser paste and fewer cracks because the amorphous gel and the particles have a higher degree of reactivity and adhesion.

Compared to heat-cured samples, ambient-cured GPC samples react slowly and require a long time to set at ambient or low temperature [159]. But heat cured samples did not show much improvement in physio-mechanical properties by incorporating SAP compared to ambient and water curing. It is due to the fact that the loss of liquid absorbed by SAP particles during mixing because of higher temperature and lower RH as discussed in section Absorption and Releasing Capabilities of SAP. The hydration reaction took place earlier and in rapid pace when GPC are cured at higher temperatures which has reduced the efficacy of SAP in heat cured specimens. However, it is necessary to acquire good strength under ambient curing in cases of practical applications.

Pore structure and pore solution resistivity both affect the electrical resistance [160]–[162]. The number and size distribution of the macro voids produced by the SAP, as well as the alteration in the capillary pore structure, have a significant impact on the electrical resistivity [89]. The level of macro void saturation is critical for electrical resistivity. When the macro voids are completely saturated, they act as an electrical conductor, and the total electrical resistance is reduced [163].

Conversely, empty macro voids act as an electrical insulator and increase electrical resistance [163].

Therefore, it can be deduced that SAP has a considerable impact on macro void saturation, leading to a decrease in electrical resistivity. Moreover, electrical resistivity in ionic solutions decreases with increasing ionic concentration, the higher electrical resistivity of R0.5 than S0.554 may be connected to the higher electrical resistivity of the pore solution of the R0.5. Previous studies have found that adding water to account for SAP absorption to PC-based composites containing SAP reduces their electrical resistivity [164], [165]. An increase in the total AA/FA ratio in the GPC may have contributed to the decrease in electrical resistivity in the pastes containing SAP. Additionally, it should be noted that ions can be constrained in SAP during absorption [166], [167], which may enhance the pore solution's electrical resistance and subsequently the GPC's electrical resistance.

Chapter 6

6. Conclusion and Recommendations

6.1   Conclusion

In this research, the effect of SAP on the workability, shrinkage, mechanical properties, and durability of fly ash based Geopolymer concrete was investigated. The absorption and release of water as well as alkaline solutions by SAP were also examined. The findings of this investigation lead to the following conclusions.

1. In comparison to water, the SAP particle exhibits a considerably diminished capacity to absorb simulated pore alkali solution. As time elapses or the temperature rises causing decline in relative humidity, the SAP gradually releases the absorbed solution.

2. At an equal total AA/FA ratio, there is a considerable reduction in both slump and density of while at an equal effective AA/FA ratio, there is slight increase in both slump and density in mix S0.554, compared to reference specimens R0.554 and R0.5, respectively.

3. The addition of 0.3% SAP by weight of fly ash resulted in a decrease in autogenous and total drying shrinkages as compared to the reference mixes. This reduction in shrinkage indicates that SAP is effective in controlling the volume change of low calcium fly ash-based GPCs.

4. The inclusion of SAP into GPCs led to an enhanced tensile and flexural strength in mix S0.554. In comparison to R0.554 at an equivalent total AA/FA ratio, the compressive strength decreased, but when compared to R0.5 at an equal effective AA/FA ratio, it improved by incorporating SAP in mix S0.554. Furthermore, SAP played a pivotal role in augmenting the strength development of GPCs.

5. The microstructure of GPC was enhanced by the incorporation of SAP due to increased geopolymerization and consumption of fly ash. SEM and XRD investigations confirmed

that the degree of geopolymerization in SAP-based GPCs was higher, which resulted in an improved physical and mechanical properties.

6. The influence of SAP on low calcium fly ash-based GPCs performance was more noticeable in ambient curing conditions than in water and heat curing. Water curing is deemed unsuitable for GPCs due to its adverse impact on both strength and durability. These results are promising and could have significant implications for the development of more durable and long-lasting GPCs.

6.2   Recommendations

SAP was found effective in reducing the shrinkage of GPCs but it induce voids which reduces the compressive strength of GPC. But these induced voids can be beneficial for GPCs at extreme temperatures. It can act as a relief zone during frezzing and thawing. Similarly at higher temperatures it can provide escape zone for vapours. So future studies have to focus on the influence of SAP on GPCs at extreme temperatures.

References

[1] M. Yazdani, M. Mojtahedi, and M. Loosemore, "Enhancing evacuation response to extreme weather disasters using public transportation systems: A novel simheuristic approach," *J. Comput. Des. Eng.*, vol. 7, no. 2, pp. 195–210, 2020, doi: 10.1093/JCDE/QWAA017.

[2] P. Mahmoudi, M. Mohammadi, and H. Daneshmand, "Investigating the trend of average changes of annual temperatures in Iran," *Int. J. Environ. Sci. Technol.*, vol. 16, no. 2, pp. 1079–1092, 2019, doi: 10.1007/s13762-018-1664-4.

[3] M. Babagolzadeh, A. Shrestha, B. Abbasi, Y. Zhang, A. Woodhead, and A. Zhang, "Sustainable cold supply chain management under demand uncertainty and carbon tax regulation," *Transp. Res. Part D Transp. Environ.*, vol. 80, p. 102245, 2020, doi: 10.1016/j.trd.2020.102245.

[4] J. Mishra, S. Das, and S. Mustakim, "Geopolymer Technology for the Promotion of Sustainable Built Environment in Future India," in *Advances in Civil Engineering (Vol. 3)*, Volume-3., AkiNik Publications, 2019, pp. 45–68.

[5] M. I. AbdulAleem and P. D. Arumairaj, "A Review of Seismic Assessment of Reinforced Concrete Structure using Pushover Analysis," *Int. J. Eng. Sci. Emerg. Technol.*, vol. 1, no. 2, pp. 118–122, 2011, doi: 10.7323/ijeset/v1.

[6] S. Kumar Karri, G. V. R. Rao, and P. M. Raju, "Strength and Durability Studies on GGBS Concrete," *Int. J. Civ. Eng.*, vol. 2, no. 10, pp. 34–41, 2015, doi: 10.14445/23488352/ijce-v2i10p106.

[7] J. Davidovits, "Geopolymer cement to minimize carbon-dioxde greenhouse-warming," *Ceram. Trans. ·*, vol. 37, no. 1, pp. 165–182, 1993, [Online]. Available: https://www.researchgate.net/publication/284682578_Geopolymer_cement_to_minimize_carbon-dioxde_greenhouse-warming.

[8] P. K. Mehta, "Greening of the Concrete Industry for Sustainable Development," *Concr. Int.*, vol. 24, no. 7, pp. 23–28, 2002.

[9] G. Fang, W. K. Ho, W. Tu, and M. Zhang, "Workability and mechanical properties of alkali-activated fly ash-slag concrete cured at ambient temperature," *Constr. Build. Mater.*, vol. 172, pp. 476–487, 2018, doi: 10.1016/j.conbuildmat.2018.04.008.

[10] F. Pacheco-Torgal, Z. Abdollahnejad, S. Miraldo, and M. Kheradmand, *Alkali-Activated Cement-Based Binders (AACBs) as Durable and Cost-Competitive Low-CO2 Binder Materials: Some Shortcomings That Need to be Addressed*. Elsevier Inc., 2017.

[11] D. Xu, Y. Cui, H. Li, K. Yang, W. Xu, and Y. Chen, "On the future of Chinese cement industry," *Cem. Concr. Res.*, vol. 78, pp. 2–13, 2015, doi: 10.1016/j.cemconres.2015.06.012.

[12] E. Benhelal, G. Zahedi, E. Shamsaei, and A. Bahadori, "Global strategies and potentials to curb CO2 emissions in cement industry," *J. Clean. Prod.*, vol. 51, pp. 142–161, 2013, doi: 10.1016/j.jclepro.2012.10.049.

[13] C. B. Cheah, L. E. Tan, and M. Ramli, "Recent advances in slag-based binder and chemical activators derived from industrial by-products – A review," *Constr. Build. Mater.*, vol. 272, no. xxxx, p. 121657, 2021, doi: 10.1016/j.conbuildmat.2020.121657.

[14] K. Jagadeeswari, S. Lal Mohiddin, K. Srinivas, and S. Kranthi Vijaya, "Mechanical characterization of alkali activated GGBS based geopolymer concrete," *Mater. Today Proc.*, no. xxxx, 2021, doi: 10.1016/j.matpr.2020.12.476.

[15] D. Hardjito, S. E. Wallah, D. M. J. Sumajouw, and B. V. Rangan, "On the development of fly ash-based geopolymer concrete," *ACI Mater. J.*, vol. 101, no. 6, pp. 467–472, 2004, doi: 10.14359/13485.

[16] P. Chindaprasirt, T. Chareerat, and V. Sirivivatnanon, "Workability and strength of coarse high calcium fly ash geopolymer," *Cem. Concr. Compos.*, vol. 29, no. 3, pp. 224–229, 2007, doi: 10.1016/j.cemconcomp.2006.11.002.

[17] M. Olivia and H. Nikraz, "Properties of fly ash geopolymer concrete designed by Taguchi method," *Mater. Des.*, vol. 36, pp. 191–198, 2012, doi: 10.1016/j.matdes.2011.10.036.

[18] K. Neupane, P. Kidd, D. Chalmers, D. Baweja, and R. Shrestha, "Investigation on compressive strength development and drying shrinkage of ambient cured powder-activated geopolymer concretes," *Aust. J. Civ. Eng.*, vol. 14, no. 1, pp. 72–83, 2016, doi: 10.1080/14488353.2016.1163765.

[19] A. Rodrigue, J. Duchesne, B. Fournier, and B. Bissonnette, "Influence of added water and fly ash content on the characteristics, properties and early-age cracking sensitivity of alkali-activated slag/fly ash concrete cured at ambient temperature," *Constr. Build. Mater.*, vol. 171, pp. 929–941, 2018, doi: 10.1016/j.conbuildmat.2018.03.176.

[20] G. Wang and Y. Ma, "Drying shrinkage of alkali-activated fly ash/slag blended system," *J. Sustain. Cem. Mater.*, vol. 7, no. 4, pp. 203–213, 2018, doi: 10.1080/21650373.2018.1471424.

[21] R. B. Ardalan, Z. N. Emamzadeh, H. Rasekh, A. Joshaghani, and B. Samali, "Physical and mechanical properties of polymer modified self-compacting concrete (SCC) using natural and recycled aggregates," *J. Sustain. Cem. Mater.*, vol. 9, no. 1, pp. 1–16, 2020, doi: 10.1080/21650373.2019.1666060.

[22] A. Kashani, T. D. Ngo, and P. Mendis, "The effects of precursors on rheology and self-compactness of geopolymer concrete," *Mag. Concr. Res.*, vol. 71, no. 11, pp. 557–566, 2019, doi: 10.1680/jmacr.17.00495.

[23] Y. J. Patel and N. Shah, "Development of self-compacting geopolymer concrete as a sustainable construction material," *Sustain. Environ. Res.*, vol. 28, no. 6, pp. 412–421, 2018, doi: 10.1016/j.serj.2018.08.004.

[24] P. Dinakar, "Design of self-compacting concrete with fly ash," *Mag. Concr. Res.*, vol. 64, no. 5, pp. 401–409, 2012, doi: 10.1680/macr.10.00167.

[25] J. L. Provis and J. S. J. van Deventer, *Binder chemistry – Blended systems and intermediate Ca content*, vol. 13. .

[26] F. Aslani and S. Nejadi, "Mechanical characteristics of self-compacting concrete with and without fibres," *Mag. Concr. Res.*, vol. 65, no. 10, pp. 608–622, 2013, doi:

10.1680/macr.12.00153.

[27] M. S. El-Feky, M. Kohail, A. M. El-Tair, and M. I. Serag, "Effect of microwave curing as compared with conventional regimes on the performance of alkali activated slag pastes," *Constr. Build. Mater.*, vol. 233, p. 117268, 2020, doi: 10.1016/j.conbuildmat.2019.117268.

[28] B. Nematollahi, J. Sanjayan, J. Qiu, and E. H. Yang, "Micromechanics-based investigation of a sustainable ambient temperature cured one-part strain hardening geopolymer composite," *Constr. Build. Mater.*, vol. 131, pp. 552–563, 2017, doi: 10.1016/j.conbuildmat.2016.11.117.

[29] J. Aliques-Granero, M. T. Tognonvi, and A. Tagnit-Hamou, "Durability study of AAMs: Sulfate attack resistance," *Constr. Build. Mater.*, vol. 229, p. 117100, 2019, doi: 10.1016/j.conbuildmat.2019.117100.

[30] L. P. Qian, Y. S. Wang, Y. Alrefaei, and J. G. Dai, "Experimental study on full-volume fly ash geopolymer mortars: Sintered fly ash versus sand as fine aggregates," *J. Clean. Prod.*, vol. 263, p. 121445, 2020, doi: 10.1016/j.jclepro.2020.121445.

[31] L.Krishnan, "Geopolymer Concrete an Eco-Friendly Construction Material," *Int. J. Res. Eng. Technol.*, vol. 03, no. 23, pp. 164–167, 2014, doi: 10.15623/ijret.2014.0323036.

[32] J. L. Provis and J. S. J. van Deventer, *Geopolymers Structure, processing, properties and industrial applications*. Woodhead Publishing Limited, Abington Hall, Granta Park, Great Abington, Cambridge CB21 6AH, UK, 2009.

[33] M. Dong, M. Elchalakani, and A. Karrech, "Development of high strength one-part geopolymer mortar using sodium metasilicate," *Constr. Build. Mater.*, vol. 236, p. 117611, 2020, doi: 10.1016/j.conbuildmat.2019.117611.

[34] F. N. Okoye, J. Durgaprasad, and N. B. Singh, "Mechanical properties of alkali activated flyash/Kaolin based geopolymer concrete," *Constr. Build. Mater.*, vol. 98, pp. 685–691, 2015, doi: 10.1016/j.conbuildmat.2015.08.009.

[35] A. F. Abdalqader, F. Jin, and A. Al-Tabbaa, "Development of greener alkali-activated cement: Utilisation of sodium carbonate for activating slag and fly ash mixtures," *J. Clean. Prod.*, vol. 113, pp. 66–75, 2016, doi: 10.1016/j.jclepro.2015.12.010.

[36] B. Nematollahi, J. Sanjayan, and F. U. A. Shaikh, "Synthesis of heat and ambient cured one-part geopolymer mixes with different grades of sodium silicate," *Ceram. Int.*, vol. 41, no. 4, pp. 5696–5704, 2015, doi: 10.1016/j.ceramint.2014.12.154.

[37] W. M. Kriven, K. . Sankar, and G. K. . Al-Chaar, "Flowable slag-fly ash binders for construction or repair," 16/255,131, 2019.

[38] M. Askarian, Z. Tao, G. Adam, and B. Samali, "Mechanical properties of ambient cured one-part hybrid OPC-geopolymer concrete," *Constr. Build. Mater.*, vol. 186, pp. 330–337, 2018, doi: 10.1016/j.conbuildmat.2018.07.160.

[39] M. N. S. Hadi, H. Zhang, and S. Parkinson, "Optimum mix design of geopolymer pastes and concretes cured in ambient condition based on compressive strength, setting time and workability," *J. Build. Eng.*, vol. 23, no. November 2018, pp. 301–313, 2019, doi: 10.1016/j.jobe.2019.02.006.

[40] G. M. Zannerni, K. P. Fattah, and A. K. Al-Tamimi, "Ambient-cured geopolymer concrete with single alkali activator," *Sustain. Mater. Technol.*, vol. 23, p. e00131, 2020, doi: 10.1016/j.susmat.2019.e00131.

[41] R. Bajpai, K. Choudhary, A. Srivastava, K. S. Sangwan, and M. Singh, "Environmental impact assessment of fly ash and silica fume based geopolymer concrete," *J. Clean. Prod.*, vol. 254, 2020, doi: 10.1016/j.jclepro.2020.120147.

[42] J. Davidovits, "Geopolymers," *J. Therm. Anal.*, vol. 37, no. 8, pp. 1633–1656, 1991, doi: 10.1007/bf01912193.

[43] C. Shi, D. Roy, and P. Krivenko, *Alkali-Activated Cements and Concretes*, 1st Editio. London, 2003.

[44] M. Nawaz, A. Heitor, and M. Sivakumar, "Geopolymers in construction - recent

developments," *Constr. Build. Mater.*, vol. 260, p. 120472, 2020, doi: 10.1016/j.conbuildmat.2020.120472.

[45]   M. C. Nataraja and L. Das, "Concrete mix proportioning as per is 10262:2009-comparison with is 10262:1982 and ACI 211.1-91," *Indian Concr. J.*, vol. 84, no. 9, pp. 64–70, 2010.

[46]   M. Ahmed, S. Islam, S. Nazar, and R. A. Khan, "A Comparative Study of Popular Concrete Mix Design Methods from Qualitative and Cost-Effective Point of View for Extreme Environment," *Arab. J. Sci. Eng.*, vol. 41, no. 4, pp. 1403–1412, 2016, doi: 10.1007/s13369-015-1946-9.

[47]   E. I. Diaz-Loya, E. N. Allouche, and S. Vaidya, "Mechanical properties of fly-ash-based geopolymer concrete," *ACI Mater. J.*, vol. 108, no. 3, pp. 300–306, 2011, doi: 10.14359/51682495.

[48]   V. B. R. Suda and P. S. Rao, "Experimental investigation on optimum usage of Micro silica and GGBS for the strength characteristics of concrete," *Mater. Today Proc.*, vol. 27, no. xxxx, pp. 805–811, 2020, doi: 10.1016/j.matpr.2019.12.354.

[49]   J. S. J. van Deventer, J. L. Provis, P. Duxson, and G. C. Lukey, "Reaction mechanisms in the geopolymeric conversion of inorganic waste to useful products," *J. Hazard. Mater.*, vol. 139, no. 3, pp. 506–513, 2007, doi: 10.1016/j.jhazmat.2006.02.044.

[50]   P. Duxson, J. L. Provis, G. C. Lukey, and J. S. J. van Deventer, "The role of inorganic polymer technology in the development of 'green concrete,'" *Cem. Concr. Res.*, vol. 37, no. 12, pp. 1590–1597, 2007, doi: 10.1016/j.cemconres.2007.08.018.

[51]   D. Hardjito and B. V. Rangan, "Development and properties of low-calcium fly ash-based geopolymer concrete," *Res. Rep. GC*, p. 94, 2005, [Online]. Available: http://www.geopolymer.org/fichiers_pdf/curtin-flyash-GP-concrete-report.pdf.

[52]   D. Khale and R. Chaudhary, "Mechanism of geopolymerization and factors influencing its development: A review," *J. Mater. Sci.*, vol. 42, no. 3, pp. 729–746, 2007, doi: 10.1007/s10853-006-0401-4.

[53] B. Singh, G. Ishwarya, M. Gupta, and S. K. Bhattacharyya, "Geopolymer concrete: A review of some recent developments," *Constr. Build. Mater.*, vol. 85, pp. 78–90, 2015, doi: 10.1016/j.conbuildmat.2015.03.036.

[54] S. Fakhrian, H. Behbahani, and S. Mashhadi, "Predicting post-fire behavior of green geopolymer mortar containing recycled concrete aggregate via gep approach," *J. Soft Comput. Civ. Eng.*, vol. 4, no. 2, pp. 22–45, 2020, doi: 10.22115/SCCE.2020.220919.1182.

[55] M. W. Hussin, M. A. R. Bhutta, M. Azreen, P. J. Ramadhansyah, and J. Mirza, "Performance of blended ash geopolymer concrete at elevated temperatures," *Mater. Struct. Constr.*, vol. 48, no. 3, pp. 709–720, 2015, doi: 10.1617/s11527-014-0251-5.

[56] D. L. Y. Kong and J. G. Sanjayan, "Effect of elevated temperatures on geopolymer paste, mortar and concrete," *Cem. Concr. Res.*, vol. 40, no. 2, pp. 334–339, 2010, doi: 10.1016/j.cemconres.2009.10.017.

[57] T. Glasby, J. Day, R. Genrich, and J. Aldred, "EFC Geopolymer Concrete Aircraft Pavements at Brisbane West Wellcamp Airport," *Concr. 2015 Conf.*, vol. 11, no. 1, pp. 1–9, 2015.

[58] J. Aldred, J. Day, and T. Glasby, "Geopolymer Concrete-No Longer Labcrete!," *40th Conf. Our World Concr. Struct. 26-28 August 2015, Singapore*, no. August, pp. 1–10, 2015, [Online]. Available: https://www.wagner.com.au/media/36779/OW15-Geopolymer-concrete-No-longer-labcrete-rev1.pdf.

[59] J. Aldred and J. Day, "Is Geopolymer Concrete a Suitable Alternative To Traditional Concrete ?," *37th Conf. Our World Concr. Struct.*, no. August, pp. 1–14, 2012.

[60] R. Bligh and T. Glasby, "Development of Geopolymer Precast Floor panels for the Global Change Institute at University of Queensland," *Concr. 2013*, pp. 1–8, 2013.

[61] A. C. Manalo, P. Mendis, Y. Bai, B. Jachmann, and C. D. Sorbello, "Fiber-Reinforced Polymer Bars for Concrete Structures: State-of-the-Practice in Australia," *J. Compos. Constr.*, vol. 25, no. 1, p. 05020007, 2021, doi: 10.1061/(asce)cc.1943-5614.0001105.

[62] S. Foster *et al.*, "Installation of Geopolymer Concrete Pavement at Wyndham Street for City of Sydney : Interim Report," pp. 9–11, 2020.

[63] J. S. J. Van Deventer, J. L. Provis, and P. Duxson, "Technical and commercial progress in the adoption of geopolymer cement," *Miner. Eng.*, vol. 29, pp. 89–104, 2012, doi: 10.1016/j.mineng.2011.09.009.

[64] S. Foster and A. Parvez, "CRC-LCL Impact Pathway 2 Summary Report : Delivering Low Carbon Materials , Products and Designs," 2019, doi: 10.13140/RG.2.2.30062.36169.

[65] A. Noushini and A. Castel, "Performance-based criteria to assess the suitability of geopolymer concrete in marine environments using modified ASTM C1202 and ASTM C1556 methods," *Mater. Struct. Constr.*, vol. 51, no. 6, 2018, doi: 10.1617/s11527-018-1267-z.

[66] J. L. Provis, "Alkali-activated materials," *Cem. Concr. Res.*, vol. 114, pp. 40–48, 2018, doi: 10.1016/j.cemconres.2017.02.009.

[67] A. McIntosh, S. E. M. Lawther, J. Kwasny, M. N. Soutsos, D. Cleland, and S. Nanukuttan, "Selection and characterisation of geological materials for use as geopolymer precursors," *Adv. Appl. Ceram.*, vol. 114, no. 7, pp. 378–385, 2015, doi: 10.1179/1743676115Y.0000000055.

[68] F.S. Andrews-Phaedonos, "Specification and use of geopolymer concrete," 2014, [Online]. Available: https://scholar.google.com/scholar_lookup?title=Sydney&author=F.S. Andrews-Phaedonos&publication_year=2014.

[69] J. . van Deventer, "Is the market ready for the adoption of alkali-activated cements," 2015.

[70] S. Foster and U. Sydney, "Project RP1020 Field Performance of Geopolymer Concrete Structures Authors."

[71] M. Lokeshwari, B. R. Pavan Bandakli, S. R. Tarun, P. Sachin, and V. Kumar, "A review on self-curing concrete," *Mater. Today Proc.*, vol. 43, pp. 2259–2264, 2020, doi:

10.1016/j.matpr.2020.12.859.

[72]   O. M. Jensen and P. F. Hansen, "Water-entrained cement-based materials: II. Experimental observations," *Cem. Concr. Res.*, vol. 32, no. 6, pp. 973–978, 2002, doi: 10.1016/S0008-8846(02)00737-8.

[73]   O. M. Jensen and P. F. Hansen, "Water-entrained cement-based materials - I. Principles and theoretical background," *Cem. Concr. Res.*, vol. 31, no. 4, pp. 647–654, 2001, doi: 10.1016/S0008-8846(01)00463-X.

[74]   S. Mönnig, "Superabsorbing additions in concrete: applications, modelling and comparison of different internal water sources," p. 180, 2009.

[75]   J. Dang, J. Zhao, and Z. Du, "Effect of superabsorbent polymer on the properties of concrete," *Polymers (Basel).*, vol. 9, no. 12, pp. 1–17, 2017, doi: 10.3390/polym9120672.

[76]   X. Zheng, M. Han, and L. Liu, "Effect of superabsorbent polymer on the mechanical performance and microstructure of concrete," *Materials (Basel).*, vol. 14, no. 12, 2021, doi: 10.3390/ma14123232.

[77]   I. Kim, S. Choi, and Y. Choi, "Effect of Internal Pores Formed by a Superabsorbent Polymer on Durability and Drying Shrinkage of Concrete Specimens," 2021.

[78]   V. Mechtcherine and H. W. Reinhardt, "Application of superabsorbent polymers (SAP) in concrete construction: State of the art report prepared by technical committee 225-SAP," *Appl. Super Absorbent Polym. Concr. Constr. State-of-the-Art Rep. Prep. by Tech. Comm. 225-SAP*, pp. 1–164, 2012, doi: 10.1007/978-94-007-2733-5.

[79]   J. Yang, F. Wang, X. He, and Y. Su, "Pore structure of affected zone around saturated and large superabsorbent polymers in cement paste," *Cem. Concr. Compos.*, vol. 97, no. June 2018, pp. 54–67, 2019, doi: 10.1016/j.cemconcomp.2018.12.020.

[80]   Y. Tan, X. Lu, R. He, H. Chen, and Z. Wang, "Influence of superabsorbent polymers (SAPs) type and particle size on the performance of surrounding cement-based materials," *Constr. Build. Mater.*, vol. 270, no. xxxx, p. 121442, 2021, doi:

10.1016/j.conbuildmat.2020.121442.

[81]   I. S. Kim, S. Y. Choi, Y. S. Choi, and E. I. Yang, "An experimental study on absorptivity measurement of superabsorbent polymers (SAP) and effect of SAP on freeze-thaw resistance in mortar specimen," *Constr. Build. Mater.*, vol. 267, no. xxxx, p. 120974, 2021, doi: 10.1016/j.conbuildmat.2020.120974.

[82]   C. Song, Y. C. Choi, and S. Choi, "Effect of internal curing by superabsorbent polymers – Internal relative humidity and autogenous shrinkage of alkali-activated slag mortars," *Constr. Build. Mater.*, vol. 123, pp. 198–206, 2016, doi: 10.1016/j.conbuildmat.2016.07.007.

[83]   W. Tu, Y. Zhu, G. Fang, X. Wang, and M. Zhang, "Internal curing of alkali-activated fly ash-slag pastes using superabsorbent polymer," *Cem. Concr. Res.*, vol. 116, no. November 2018, pp. 179–190, 2019, doi: 10.1016/j.cemconres.2018.11.018.

[84]   Y. Wang, L. Montanari, W. Jason Weiss, and P. Suraneni, "Internal Curing Using Superabsorbent Polymers for Alkali Activated Slag-Fly Ash Mixtures BT - 3rd International Conference on the Application of Superabsorbent Polymers (SAP) and Other New Admixtures Towards Smart Concrete," 2020, pp. 239–247.

[85]   Z. Li, X. Yao, Y. Chen, T. Lu, and G. Ye, "A low-autogenous-shrinkage alkali-activated slag and fly ash concrete," *Appl. Sci.*, vol. 10, no. 17, 2020, doi: 10.3390/app10176092.

[86]   S. Oh and Y. C. Choi, "Superabsorbent polymers as internal curing agents in alkali activated slag mortars," *Constr. Build. Mater.*, vol. 159, pp. 1–8, 2018, doi: 10.1016/j.conbuildmat.2017.10.121.

[87]   B. Vafaei, K. Farzanian, and A. Ghahremaninezhad, "The influence of superabsorbent polymer on the properties of alkali-activated slag pastes," *Constr. Build. Mater.*, vol. 236, p. 117525, 2020, doi: 10.1016/j.conbuildmat.2019.117525.

[88]   D. Jiang *et al.*, "Autogenous shrinkage and hydration property of alkali activated slag pastes containing superabsorbent polymer," *Cem. Concr. Res.*, vol. 149, no. April, p. 106581, 2021, doi: 10.1016/j.cemconres.2021.106581.

[89] J. Prabahar, B. Vafaei, and A. Ghahremaninezhad, "The Effect of Hydrogels with Different Chemical Compositions on the Behavior of Alkali-Activated Slag Pastes," *Gels*, 2022.

[90] P. Wang *et al.*, "Effect of internal curing by super absorbent polymer on the autogenous shrinkage of alkali-activated slag mortars," *Materials (Basel).*, vol. 13, no. 19, pp. 1–13, 2020, doi: 10.3390/ma13194318.

[91] Z. Yang, P. Shi, Y. Zhang, and Z. Li, "Influence of liquid-binder ratio on the performance of alkali-activated slag mortar with superabsorbent polymer," *J. Build. Eng.*, vol. 48, no. December 2021, p. 103934, 2022, doi: 10.1016/j.jobe.2021.103934.

[92] J. Yang, D. Snoeck, N. De Belie, and Z. Sun, "Effect of superabsorbent polymers and expansive additives on the shrinkage of alkali-activated slag," *Cem. Concr. Compos.*, vol. 123, no. June, p. 104218, 2021, doi: 10.1016/j.cemconcomp.2021.104218.

[93] Z. Yang, P. Shi, Y. Zhang, and Z. Li, "Effect of superabsorbent polymer introduction on properties of alkali-activated slag mortar," *Constr. Build. Mater.*, vol. 340, no. August 2021, p. 127541, 2022, doi: 10.1016/j.conbuildmat.2022.127541.

[94] S. Afridi, M. A. Sikandar, M. Waseem, H. Nasir, and A. Naseer, "Chemical durability of superabsorbent polymer (SAP) based geopolymer mortars (GPMs)," *Constr. Build. Mater.*, vol. 217, pp. 530–542, 2019, doi: 10.1016/j.conbuildmat.2019.05.101.

[95] W. Khaliq and W. Javaid, "Characterization of conventional and modern curing techniques in concrete," *Key Eng. Mater.*, vol. 711, pp. 1118–1125, 2016, doi: 10.4028/www.scientific.net/KEM.711.1118.

[96] P. Zhong, Z. Hu, M. Griffa, M. Wyrzykowski, J. Liu, and P. Lura, "Mechanisms of internal curing water release from retentive and non-retentive superabsorbent polymers in cement paste," *Cem. Concr. Res.*, vol. 147, no. May, p. 106494, 2021, doi: 10.1016/j.cemconres.2021.106494.

[97] A. M. Soliman and M. L. Nehdi, "Effect of drying conditions on autogenous shrinkage in ultra-high performance concrete at early-age," *Mater. Struct. Constr.*, vol. 44, no. 5, pp.

879–899, 2011, doi: 10.1617/s11527-010-9670-0.

[98]   X. ming Kong, Z. lin Zhang, and Z. chen Lu, "Effect of pre-soaked superabsorbent polymer on shrinkage of high-strength concrete," *Mater. Struct. Constr.*, vol. 48, no. 9, pp. 2741–2758, 2015, doi: 10.1617/s11527-014-0351-2.

[99]   X. Ma, J. Liu, Z. Wu, and C. Shi, "Effects of SAP on the properties and pore structure of high performance cement-based materials," *Constr. Build. Mater.*, vol. 131, pp. 476–484, 2017, doi: 10.1016/j.conbuildmat.2016.11.090.

[100] S. Zhutovsky and K. Kovler, "Influence of water to cement ratio on the efficiency of internal curing of high-performance concrete," *Constr. Build. Mater.*, vol. 144, pp. 311–316, 2017, doi: 10.1016/j.conbuildmat.2017.03.203.

[101] S. H. Kang, S. G. Hong, and J. Moon, "Importance of drying to control internal curing effects on field casting ultra-high performance concrete," *Cem. Concr. Res.*, vol. 108, no. October 2017, pp. 20–30, 2018, doi: 10.1016/j.cemconres.2018.03.008.

[102] E. Silva, M. Alejandro, R. Manzano, R. Dias, and T. Filho, "EFFECT OF SAP ON THE AUTOGENOUS SHRINKAGE AND COMPRESSIVE STRENGTH OF HIGH-STRENGTH FINE-GRAINED CONCRETE EFFECT OF SAP ON THE AUTOGENOUS SHRINKAGE AND COMPRESSIVE STRENGTH OF HIGH-STRENGTH FINE-GRAINED CONCRETE Eletrobras Furnas Hydroelectric Company , G," no. May, 2020.

[103] J. Liu, N. Farzadnia, and C. Shi, "Effects of superabsorbent polymer on interfacial transition zone and mechanical properties of ultra-high performance concrete," *Constr. Build. Mater.*, vol. 231, p. 117142, 2020, doi: 10.1016/j.conbuildmat.2019.117142.

[104] J. Liu, N. Farzadnia, K. H. Khayat, and C. Shi, "Effects of SAP characteristics on internal curing of UHPC matrix," *Constr. Build. Mater.*, vol. 280, p. 122530, 2021, doi: 10.1016/j.conbuildmat.2021.122530.

[105] S. A. Mudashiru, 1a, B. J. Olawuyi, 1b, S. T. Ayegbokiki, and S. K. Ndayako, "Influence of Magnesium Sulphate on the Compressive Strength of Internal Cured (IC) Rice Husk

Ash based High Performance Concrete," no. May, p., 2021.

[106] M. Y. Xuan, Y. S. Wang, X. Y. Wang, H. S. Lee, and S. J. Kwon, "Effect of cement types and superabsorbent polymers on the properties of sustainable ultra-high-performance paste," *Materials (Basel).*, vol. 14, no. 6, pp. 1–20, 2021, doi: 10.3390/ma14061497.

[107] B. J. Olawuyi, A. J. Babafemi, and W. P. Boshoff, "Early-age and long-term strength development of high-performance concrete with SAP," *Constr. Build. Mater.*, vol. 267, p. 121798, 2021, doi: 10.1016/j.conbuildmat.2020.121798.

[108] J. Liu, N. Farzadnia, and C. Shi, "Microstructural and micromechanical characteristics of ultra-high performance concrete with superabsorbent polymer (SAP)," *Cem. Concr. Res.*, vol. 149, no. July, 2021, doi: 10.1016/j.cemconres.2021.106560.

[109] Z. Li, S. Zhang, X. Liang, J. Granja, M. Azenha, and G. Ye, "Internal curing of alkali-activated slag-fly ash paste with superabsorbent polymers," *Constr. Build. Mater.*, vol. 263, p. 120985, 2020, doi: 10.1016/j.conbuildmat.2020.120985.

[110] Z. Li *et al.*, "Internal curing by superabsorbent polymers in alkali-activated slag," *Cem. Concr. Res.*, vol. 135, no. May, p. 106123, 2020, doi: 10.1016/j.cemconres.2020.106123.

[111] C. Fu, H. Ye, A. Lei, G. Yang, and P. Wan, "Effect of novel superabsorbent polymer composites on the fresh and hardened properties of alkali-activated slag," *Constr. Build. Mater.*, vol. 232, p. 117225, 2020, doi: 10.1016/j.conbuildmat.2019.117225.

[112] J. Yang, D. Snoeck, N. De Belie, and Z. Sun, "Comparison of liquid absorption-release of superabsorbent polymers in alkali-activated slag and Portland cement systems: An NMR study combined with additional methods," *Cem. Concr. Res.*, vol. 142, no. August 2020, p. 106369, 2021, doi: 10.1016/j.cemconres.2021.106369.

[113] M. A. Uddin, A. W. Akbar, M. Ahmed, and M. F. Ali, "Strength and Durability Study on Fly-ash Concrete Blended with Superabsorbent Polymer," pp. 1416–1421, 2020.

[114] L. Rajamony Laila, B. G. A. Gurupatham, K. Roy, and J. B. P. Lim, "Effect of super absorbent polymer on microstructural and mechanical properties of concrete blends using

granite pulver," *Struct. Concr.*, vol. 22, no. S1, pp. E898–E915, 2021, doi: 10.1002/suco.201900419.

[115] ASTM C 618, "Standard Specification for Coal Fly Ash and Raw or Calcined Natural Pozzolan for Use in Concrete, ASTM International, West Conshohocken, PA, 2012, www.astm.org," *ASTM Int.*, pp. 1–5, 2014, doi: 10.1520/C0618.

[116] A. Fernández-Jiménez and A. Palomo, "Characterisation of fly ashes. Potential reactivity as alkaline cements," *Fuel*, vol. 82, no. 18, pp. 2259–2265, 2003, doi: 10.1016/S0016-2361(03)00194-7.

[117] ASTM C127, "Standard Test Method for Specific Gravity and Water Absorption of Coarse Aggregate," *Am. Soc. Test. Mater.*, vol. 04, no. Reapproved, pp. 1–6, 2001.

[118] ASTM International, "ASTM C136/C136M Standard Test Method for Sieve Analysis of Fine and Coarse Aggregates," *ASTM Stand. B.*, pp. 3–7, 2019.

[119] ASTM C128, "Standard Test Method for Relative Density (Specific Gravity) and Absorption of Fine Aggregates, ASTM International, West Conshohocken, PA, 2015," *ASTM Int.*, vol. i, pp. 15–20, 2015, [Online]. Available: www.astm.org.

[120] M. T. Ghafoor, Q. S. Khan, A. U. Qazi, M. N. Sheikh, and M. N. S. Hadi, "Influence of alkaline activators on the mechanical properties of fly ash based geopolymer concrete cured at ambient temperature," *Constr. Build. Mater.*, vol. 273, p. 121752, 2021, doi: 10.1016/j.conbuildmat.2020.121752.

[121] J. Liu, N. Farzadnia, C. Shi, and X. Ma, "Effects of superabsorbent polymer on shrinkage properties of ultra-high strength concrete under drying condition," *Constr. Build. Mater.*, vol. 215, pp. 799–811, 2019, doi: 10.1016/j.conbuildmat.2019.04.237.

[122] C. Schröfl, V. Mechtcherine, and M. Gorges, "Relation between the molecular structure and the efficiency of superabsorbent polymers (SAP) as concrete admixture to mitigate autogenous shrinkage," *Cem. Concr. Res.*, vol. 42, no. 6, pp. 865–873, 2012, doi: 10.1016/j.cemconres.2012.03.011.

[123] D. Snoeck, C. Schröfl, and V. Mechtcherine, "Recommendation of RILEM TC 260-RSC: testing sorption by superabsorbent polymers (SAP) prior to implementation in cement-based materials," *Mater. Struct. Constr.*, vol. 51, no. 5, 2018, doi: 10.1617/s11527-018-1242-8.

[124] V. Mechtcherine *et al.*, "Testing superabsorbent polymer (SAP) sorption properties prior to implementation in concrete: results of a RILEM Round-Robin Test," *Mater. Struct. Constr.*, vol. 51, no. 1, 2018, doi: 10.1617/s11527-018-1149-4.

[125] ASTM: C143/C143M − 12, "Standard Test Method for Slump of Hydraulic cement concrete," *ASTM Int.*, vol. i, no. Reapproved, pp. 1–4, 2014, doi: 10.1520/C0143.

[126] ASTM: C138/C138M − 13, "Standard Test Method for Density (Unit Weight), Yield, and Air Content (Gravimetric)," *ASTM Int.*, vol. i, pp. 23–26, 2013, doi: 10.1520/C0138.

[127] ASTM: C642, "Standard Test Method for Density, Absorption, and Voids in Hardened Concrete, ASTM International, United States," *Annu. B. ASTM Stand.*, no. March, pp. 1–3, 2013.

[128] ASTM: C39/C39M, "Standard Test Method for Compressive Strength of Cylindrical Concrete Specimens 1," *ASTM Stand. B.*, vol. i, no. March, pp. 1–5, 2003.

[129] ASTM C923/C293M, "ASTM Standards C 293-02," *Stand. Test Method Flexural Strength Concr. (Using Simple Beam With Center-Point Loading)*, pp. 1–3, 2002, [Online]. Available: https://normanray.files.wordpress.com/2010/10/kuliah-7-c293.pdf.

[130] ASTM: C496/C496M − 17, "Standard Test Method for Splitting Tensile Strength of Cylindrical Concrete Specimens ASTM C-496," *ASTM Int.*, no. March 1996, pp. 1–5, 2011, [Online]. Available: ftp://ftp.astmtmc.cmu.edu/docs/diesel/cummins/procedure_and_ils/ism/Archive/ISM Procedure (Draft 10).doc.

[131] ASTM C 157/C 157M–17, "Standard Test Method for Length Change of Hardened Hydraulic-Cement Mortar and," *Annu. B. ASTM Stand.*, vol. 04, pp. 1–7, 2017.

[132] K. Mermerdaş, Z. Algın, and Ekmen, "Experimental assessment and optimization of mix parameters of fly ash-based lightweight geopolymer mortar with respect to shrinkage and strength," *J. Build. Eng.*, vol. 31, no. November 2019, 2020, doi: 10.1016/j.jobe.2020.101351.

[133] C. C. Test, M. Cabinets, M. Rooms, C. C. Test, T. Drilled, and C. Ag-, "ASTM Standard C1760 - Standard Test Method for Bulk Electrical Conductivity of Hardened Concrete," *ASTM Int.*, vol. i, no. c, pp. 1–5, 2012, doi: 10.1520/C1876-19.

[134] S. C. Gebhard, D. A. Gratson, R. J. French, M. A. Ratcliff, J. A. Patrick, and M. A. Paisley, "I 1048," *DIN 1048-5 Test. Concr. Test. Hardened Concr.*, no. 0106, 1991.

[135] American Society for Testing and Material, "ASTM C 597-02, Standard test Method For Pulse Velocity Through Concrete," *United States Am. Soc. Test. Mater.*, vol. 04, no. 02, pp. 3–6, 2003.

[136] ASTM: E1508 − 98, "Standard Guide for Quantitative Analysis by Energy-Dispersive Spectroscopy," *Annu. B. ASTM Stand.*, vol. 98, no. Reapproved, pp. 1–8, 2003.

[137] ASTM: C1723 − 10, "Standard Guide for Examination of Hardened Concrete Using Scanning Electron Microscopy," *Annu. B. ASTM Stand.*, no. Reapproved 2004, pp. 1–17, 2011, doi: 10.1520/C1723-10.Copyright.

[138] B. A. Salami, M. A. Megat Johari, Z. A. Ahmad, and M. Maslehuddin, "Impact of added water and superplasticizer on early compressive strength of selected mixtures of palm oil fuel ash-based engineered geopolymer composites," *Constr. Build. Mater.*, vol. 109, pp. 198–206, 2016, doi: 10.1016/j.conbuildmat.2016.01.033.

[139] ACI 318, *Building Code Requirements for Structural Concrete*. 2014.

[140] W. Chen, B. Li, J. Wang, and N. Thom, "Effects of alkali dosage and silicate modulus on autogenous shrinkage of alkali-activated slag cement paste," *Cem. Concr. Res.*, vol. 141, no. October 2020, 2021, doi: 10.1016/j.cemconres.2020.106322.

[141] P. Lura, O. M. Jensen, and J. Weiss, "Cracking in cement paste induced by autogenous

shrinkage," *Mater. Struct. Constr.*, vol. 42, no. 8, pp. 1089–1099, 2009, doi: 10.1617/s11527-008-9445-z.

[142] C. Arya, "Eurocode 2: Design of concrete structures," *Des. Struct. Elem.*, vol. 3, no. July, pp. 334–394, 2015, doi: 10.1201/b18121-18.

[143] M. T. Hasholt, O. M. Jensen, K. Kovler, and S. Zhutovsky, "Can superabsorent polymers mitigate autogenous shrinkage of internally cured concrete without compromising the strength?," *Constr. Build. Mater.*, vol. 31, pp. 226–230, 2012, doi: 10.1016/j.conbuildmat.2011.12.062.

[144] D. Snoeck, D. Schaubroeck, P. Dubruel, and N. De Belie, "Effect of high amounts of superabsorbent polymers and additional water on the workability, microstructure and strength of mortars with a water-to-cement ratio of 0.50," *Constr. Build. Mater.*, vol. 72, pp. 148–157, 2014, doi: 10.1016/j.conbuildmat.2014.09.012.

[145] A. H. Mahmood, S. J. Foster, and A. Castel, "Effects of mixing duration on engineering properties of geopolymer concrete," *Constr. Build. Mater.*, vol. 303, no. August, p. 124449, 2021, doi: 10.1016/j.conbuildmat.2021.124449.

[146] S. M. Nyale, O. O. Babajide, G. D. Birch, N. Böke, and L. F. Petrik, "Synthesis and Characterization of Coal Fly Ash-based Foamed Geopolymer," *Procedia Environ. Sci.*, vol. 18, pp. 722–730, 2013, doi: 10.1016/j.proenv.2013.04.098.

[147] F. Puertas, A. Fernández-Jiménez, and M. T. Blanco-Varela, "Pore solution in alkali-activated slag cement pastes. Relation to the composition and structure of calcium silicate hydrate," *Cem. Concr. Res.*, vol. 34, no. 1, pp. 139–148, 2004, doi: 10.1016/S0008-8846(03)00254-0.

[148] S. A. Bernal *et al.*, "Gel nanostructure in alkali-activated binders based on slag and fly ash, and effects of accelerated carbonation," *Cem. Concr. Res.*, vol. 53, pp. 127–144, 2013, doi: 10.1016/j.cemconres.2013.06.007.

[149] A. Vorgelegt, J. Hauptberichter, and H. R. Mitberichter, "Superabsorbing additions in concrete – applications , modelling and," 2009.

[150] P. Lura, O. M. Jensen, and K. van Breugel, "Autogenous shrinkage in high-performance cement paste: An evaluation of basic mechanisms," *Cem. Concr. Res.*, vol. 33, no. 2, pp. 223–232, 2003, doi: https://doi.org/10.1016/S0008-8846(02)00890-6.

[151] M. Collepardi, A. Borsoi, S. Collepardi, J. J. Ogoumah Olagot, and R. Troli, "Effects of shrinkage reducing admixture in shrinkage compensating concrete under non-wet curing conditions," *Cem. Concr. Compos.*, vol. 27, no. 6, pp. 704–708, 2005, doi: 10.1016/j.cemconcomp.2004.09.020.

[152] H. Ye and A. Radlińska, "A Review and Comparative Study of Existing Shrinkage Prediction Models for Portland and Non-Portland Cementitious Materials," *Adv. Mater. Sci. Eng.*, vol. 2016, pp. 10–14, 2016, doi: 10.1155/2016/2418219.

[153] A. Radlinska, F. Rajabipour, B. Bucher, R. Henkensiefken, G. Sant, and J. Weiss, "Shrinkage mitigation strategies in cementitious systems: A closer look at differences in sealed and unsealed behavior," *Transp. Res. Rec.*, no. 2070, pp. 59–67, 2008, doi: 10.3141/2070-08.

[154] K. K. Poloju and K. Srinivasu, "Impact of GGBS and strength ratio on mechanical properties of geopolymer concrete under ambient curing and oven curing," *Mater. Today Proc.*, vol. 42, pp. 962–968, 2020, doi: 10.1016/j.matpr.2020.11.934.

[155] O. A. Mayhoub, E. S. A. R. Nasr, Y. Ali, and M. Kohail, "Properties of slag based geopolymer reactive powder concrete," *Ain Shams Eng. J.*, vol. 12, no. 1, pp. 99–105, 2021, doi: 10.1016/j.asej.2020.08.013.

[156] B. A. Ionescu, A.-V. Lăzărescu, and A. Hegyi, "The Possibility of Using Slag for the Production of Geopolymer Materials and Its Influence on Mechanical Performances—A Review," in *Interdisciplinarity in Engineering*, 2020, p. 30, doi: 10.3390/proceedings2020063030.

[157] Saloni, A. Singh, V. Sandhu, Jatin, and Parveen, "Effects of alccofine and curing conditions on properties of low calcium fly ash-based geopolymer concrete," *Mater. Today Proc.*, vol. 32, no. xxxx, pp. 620–625, 2020, doi: 10.1016/j.matpr.2020.02.763.

[158] Z. Abdollahnejad, A. Dalvand, M. Mastali, T. Luukkonen, and M. Illikainen, "Effects of waste ground glass and lime on the crystallinity and strength of geopolymers," *Mag. Concr. Res.*, vol. 71, no. 23, pp. 1218–1231, 2019, doi: 10.1680/jmacr.18.00300.

[159] P. Nath, P. K. Sarker, and V. B. Rangan, "Early age properties of low-calcium fly ash geopolymer concrete suitable for ambient curing," *Procedia Eng.*, vol. 125, pp. 601–607, 2015, doi: 10.1016/j.proeng.2015.11.077.

[160] Y. Bu and J. Weiss, "The influence of alkali content on the electrical resistivity and transport properties of cementitious materials," *Cem. Concr. Compos.*, vol. 51, pp. 49–58, 2014, doi: 10.1016/j.cemconcomp.2014.02.008.

[161] J. Jain and N. Neithalath, "Electrical impedance analysis based quantification of microstructural changes in concretes due to non-steady state chloride migration," *Mater. Chem. Phys.*, vol. 129, no. 1–2, pp. 569–579, 2011, doi: 10.1016/j.matchemphys.2011.04.057.

[162] N. Neithalath, J. Weiss, and J. Olek, "Characterizing Enhanced Porosity Concrete using electrical impedance to predict acoustic and hydraulic performance," *Cem. Concr. Res.*, vol. 36, no. 11, pp. 2074–2085, 2006, doi: 10.1016/j.cemconres.2006.09.001.

[163] H. S. Wong, A. M. Pappas, R. W. Zimmerman, and N. R. Buenfeld, "Effect of entrained air voids on the microstructure and mass transport properties of concrete," *Cem. Concr. Res.*, vol. 41, no. 10, pp. 1067–1077, 2011, doi: 10.1016/j.cemconres.2011.06.013.

[164] Y. Wehbe and A. Ghahremaninezhad, "Combined effect of shrinkage reducing admixtures (SRA) and superabsorbent polymers (SAP) on the autogenous shrinkage, hydration and properties of cementitious materials," *Constr. Build. Mater.*, vol. 138, pp. 151–162, 2017, doi: 10.1016/j.conbuildmat.2016.12.206.

[165] M. Kamali and A. Ghahremaninezhad, "An investigation into the influence of superabsorbent polymers on the properties of glass powder modified cement pastes," *Constr. Build. Mater.*, vol. 149, pp. 236–247, 2017, doi: 10.1016/j.conbuildmat.2017.04.125.

[166] J. Justs, M. Wyrzykowski, F. Winnefeld, D. Bajare, and P. Lura, "Influence of superabsorbent polymers on hydration of cement pastes with low water-to-binder ratio: A calorimetry study," *J. Therm. Anal. Calorim.*, vol. 115, no. 1, pp. 425–432, 2014, doi: 10.1007/s10973-013-3359-x.

[167] W. Siriwatwechakul, J. Siramanont, and W. Vichit-Vadakan, "Behavior of Superabsorbent Polymers in Calcium- and Sodium-Rich Solutions," *J. Mater. Civ. Eng.*, vol. 24, no. 8, pp. 976–980, 2012, doi: 10.1061/(asce)mt.1943-5533.0000449.